Research Article

Tectono-sedimentary processes shaping the West Sardinian margin and adjacent oceanic basin during the Plio-Quaternary (Western Mediterranean Sea)

Veronica Frisicchio [a,*], Anna Del Ben [a], Riccardo Geletti [b], Maria Cristina Caradonna [a], Michele Rebesco [b], Massimo Bellucci [c]

[a] *Department of Mathematics, Informatics and Geosciences, University of Trieste, Via Weiss, 1, 34128 Trieste, Italy*
[b] *National Institute of Oceanography and Applied Geophysics – OGS Borgo Grotta Gigante 42/C, 34010 Sgonico, Trieste, Italy*
[c] *Geo-Ocean, Univ Brest, CNRS, Ifremer, UMR6538, F-29280 Plouzane, France*

ARTICLE INFO

ABSTRACT

A seismic analysis of the Plio-Quaternary stratigraphy of the West Sardinian continental margin and adjacent oceanic basin was conducted using single- and multi-channel seismic profiles. Two main chronostratigraphic boundaries have been used: i) the Ms horizon, marking the base of the Pliocene and corresponding to the top of the Messinian evaporites on the lower continental slope and deep basin, and the Messinian erosional truncation on the upper slope and shelf; and ii) the newly identified A_0 horizon, marking the base of the Quaternary (2.6 Ma). This study reveals key geological features affecting the Pliocene and Quaternary deposits: a) salt tectonic structures, b) normal faults, c) volcanic structures, d) pockmarks, e) canyon systems, and f) regressive clinoform system. These features are linked to tectono-sedimentary processes such as vertical movements, magmatic activity, halokinesis and sediment dynamics. Vertical movements are associated with the thermal subsidence of the Oligo-Miocene basin opening, water and sediment loading/unloading during and after the Messinian Salinity Crisis, and Pleistocene uplift onshore. These movements resulted in the tilting of the margin, which influenced normal faulting through reactivation of Oligo-Miocene faults, and the Plio-Quaternary depositional patterns. Several normal faults acted as conduits for lower Pliocene magmatic activity and gas migration, forming volcanoes and pockmarks on the continental shelf and upper slope. Salt tectonics in the lower slope and deep basin produced diapirs and rollover structures, significantly impacting the thickness and distribution of Pliocene and, to a lesser extent, Quaternary deposits. Canyons system formation seems to be controlled by the interplay of the Quaternary sea-level fluctuations with the margin's ongoing tilting. Similarly, the regressive clinoform system also results from these two factors, but is further influenced by erosion of uplifted Sardinian onshore areas.

1. Introduction

The West Sardinian passive continental margin, in the Western Mediterranean Sea (Fig. 1a), originated during the upper Oligocene-lower Miocene (uO-lM) rifting and drifting of the Sardo-Provençal Basin. Several studies have shed light on its geodynamic evolution (Cherchi and Montadert, 1982; Fais et al., 1996; Casula et al., 2001; Faccenna et al., 2002; Finetti et al., 2005; Gattacceca et al., 2007; Carminati et al., 2012) and the effect of the Messinian Salinity Crisis (MSC)

and related salt morphologies, explored by Lofi et al. (2011), Geletti et al. (2014), Dal Cin et al. (2015), Del Ben et al. (2018), Bellucci et al. (2021a). Some authors analyzed the Plio-Quaternary (PQ) seismic facies (Sage et al., 2005; Geletti et al., 2014; Dal Cin et al., 2015) and the Pliocene magmatism of the Catalano Volcanic Field (CVF) (Conforti et al., 2016). The difference in seismic facies between the Pliocene and Quaternary is widely recognized in other margins of the West Mediterranean Sea, such as the Tyrrhenian Sea (Selli and Fabbri, 1971; Fabbri and Nanni, 1980; Mauffret et al., 1999), Sicily Channel (Civile et al.,

---

2014), Alboran Sea (Juan et al., 2016; Ercilla et al., 2022), Ionian Sea (Volpi et al., 2017 and references therein), Gulf of Lion (Leroux et al., 2017) and Adriatic Sea (Špelić et al., 2021 and references therein). On the contrary, there is a lack of detailed seismic studies about the PQ stratigraphy and its facies and relationship with geologic structures in the West Sardinian margin. In this study, we present a new interpretation of the PQ sequence of this margin and adjacent basin, focusing on the tectono-sedimentary processes that have shaped the region over the last 5.3 million years, with special attention to the influence of earlier events, particularly the MSC. By analyzing the PQ sequence stratigraphy, distinguished by their different seismic facies, we explore the shallower structures of the margin and document the geological events affecting them during Pliocene and Quaternary times.

2. Geological framework

The West Sardinian passive margin, located in the Western Mediterranean Sea (Fig. 1a), structured following the opening of the Sardo-Provençal basin (Fig. 1a), between 30 and 15 Ma (Cherchi and

Montadert, 1982; Rehault et al., 1984; Dewey et al., 1989; Rosenbaum et al., 2002; Carminati et al., 2012; Lustrino et al., 2013). This period was characterized by calc-alkaline volcanism, associated with subduction, which spread both onshore and offshore throughout the basin extension (Franciosi et al., 2003; Gattacceca et al., 2007; Lustrino et al., 2007a, 2007b, 2013). More recent sodic-alkaline magmatic activity in the Corso-Sardinian block (Lustrino et al., 2013) began during the Messinian (Casula et al., 2001), continuing through the Pliocene (Geletti et al., 2014; Conforti et al., 2016), and into the late Quaternary (Conforti et al., 2016), as evidenced by the Catalano Volcanic Field (CVF) in the continental shelf (Conforti et al., 2016).

The region's fracture systems (Torelli et al., 1990; Bigi et al., 1992a, 1992b; Fais et al., 1996; Faccenna et al., 2002; Sage et al., 2005; Oudet et al., 2010) are primarily associated with the uO-lM extensional tectonics (Cherchi and Montadert, 1982; Rehault et al., 1984; Fais et al., 1996; Ferrandini et al., 2003; Gattacceca et al., 2007). The Oligo-Miocene (OM) sedimentary sequence filled and covered the horst and graben structures that originated during the rifting and drifting phases of the Sardo-Provençal basin opening (Cherchi et al., 1982; Fais et al.,
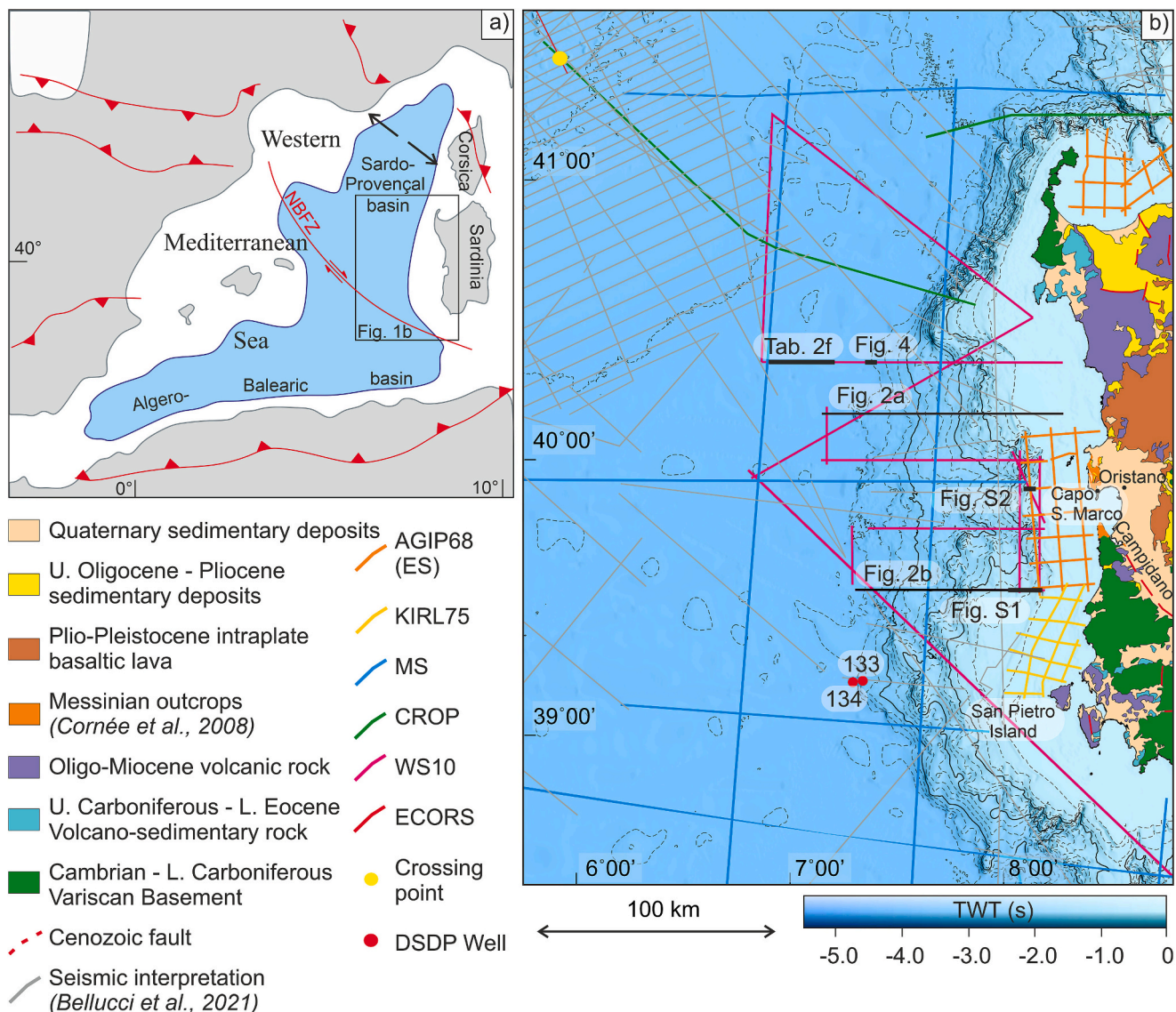

Fig. 1. Location of the study area. a) The Sardo-Provençal basin is located in the Western Mediterranean Sea and opened following the anticlockwise rotation of the Corso-Sardinian block along the North Balearic Fracture Zone (NBFZ); b) Zoom of the study area with position of the data used. The grey lines represent the position of profiles used by Bellucci et al. (2021b), whose data were integrated in this paper. Bathymetry from "EMODnet bathymetry", time-converted using a mean velocity of 1500 m/s: bold lines every 1 s, dashed lines every 0.25 s. Land geology is from Carmignani et al., 2016.

1996; Geletti et al., 2014). This sequence was later involved in the MSC (Rehault et al., 1984; Cherchi et al., 2008; Geletti et al., 2014), which was triggered by the closure of the Betic (Iberian) and Rifian (Morocco) corridors and the consequent separation of the Mediterranean Sea from the Atlantic Ocean (Clauzon et al., 1996; Krijgsman et al., 1999; CIESM, 2008). This led to the deposition of a 1600–2100 m thick evaporite sequence in deep basins, typically classified into three units (Rehault et al., 1984): Lower Unit (LU), Mobile Unit (MU, i.e., the salt) and Upper Unit (UU) (Sage et al., 2005; Lofi et al., 2008, 2011; Lofi, 2018; Geletti et al., 2014; Dal Cin et al., 2015; Del Ben et al., 2018). In the upper continental slope and shelf, the main evidence of the MSC is the Messinian Erosional Surface (MES), a high-amplitude marker, often identified by the truncation of the pre-Messinian layers describing a clear angular discordance with the overlying Pliocene conformable layers (Clauzon et al., 1996). The MES is generally rugged on the shelf, becoming smoother basinward (Lofi et al., 2007, 2011; Lofi, 2018) and is commonly interpreted as the result of subaerial erosion, by river action or retrogressive erosion (Loget and Van Den Driessche, 2006; Lofi et al., 2007; Estrada et al., 2011). Several investigations have identified Messinian paleo-fluvial networks on other margins of the Western Mediterranean Sea, such as the Gulf of Lions shelf, Ebro margins, Valencia trough and Alboran Sea (Stampfli and Höcker, 1989; Guennoc et al., 2000; Lofi et al., 2007; Estrada et al., 2011; Pellen et al., 2019). In addition, recent canyons systems, associated to the MSC by Harris and Whiteway (2011), have been identified on the West Sardinian margin (Ulzega, 1988). The deposition of the PQ sequence began after the reopening of the Strait of Gibraltar, when marine conditions were reestablished (Hsü et al., 1973; Lofi et al., 2005). The PQ sequence lies above pre-Messinian units on the continental shelf and slope and above the MSC units in the deep basin. It is characterized by a deeper marly facies of low seismic amplitude and a shallower facies of high amplitude, including turbidite deposits (Geletti et al., 2014). On the continental margins, only the lower facies of the PQ sequence are typically present, often deformed by salt structures, where present (Dal Cin et al., 2015), while the complete sequence is preserved in the deep adjacent basin (Geletti et al., 2014).

The West Sardinian margin remained tectonically stable during the Messinian (Sage et al., 2005). However, since the Pliocene, extensional activity occurred in the Campidano Graben (Fig. 1b), which has been related to the east-ward moving Tyrrhenian mantle flux (Finetti et al., 2005). This younger graben, partly superimposed on the OM Sardinian rift system (Casula et al., 2001), has influenced the West Sardinian margin reaching the Gulf of Oristano.

3. Data and methods

3.1. Data

We used 2D reflection seismic lines from multiple surveys, with different resolutions, acquired between 1968 and 2010 (Table 1). These were integrated with the seismic interpretation of Bellucci et al. (2021b)

Table 1
Parameters of the interpreted seismic data.

Seismic survey	Year of acquisition	Source	Streamer length	Sample rate	Data length
WS10 project	2010	2 Gi-Gun (11.6 l)	1500 m	1 ms	8 s
AGIP68 (ES)	1968	Aquapulse	1600 m	2 ms	4 s
KIRL75	1975	Vaporchoc	2400 m	2 ms	4 s
MS project	1969–1973	3 guns (Flexotir)	2400 m	4 ms	6 to 10 s
CROP project (M1, M2A1)	1988–1995	Air Gun (80 l)	3000/ 4500 m	4 ms	16/17 s

for the deep basin (Fig. 1b). The primary dataset used in this work consists of the WS10 seismic profiles, acquired in 2010 by the National Institute of Oceanography and Applied Geophysics-OGS (Zgur et al., 2010; Geletti et al., 2014) to explore the western and southern margins of Sardinia. These medium resolution profiles provide detailed insights into the Messinian and PQ units. Additionally, seismic reflection lines AGIP68 (ES) and KIRL75, freely available on the ViDEPI (2009) website database, offer extensive coverage of the continental shelf. The ES dataset was acquired in 1968 by the Western Geophysical Co. for the Agip oil company as part of an Italian government exploration project, while the KIRL 75 dataset was acquired by Kilroy of Texas in 1975. The MS project, also acquired by OGS, took place between 1969 and 1973 and covers the Mediterranean region. The CROP project (1988–1995), a multidisciplinary research project, provides high penetration seismic lines, reaching the lithosphere. The MS and CROP profiles improve the 2D seismic coverage and allow the correlation of the PQ features with the deepest and oldest structures. The bathymetric data come from EMODnet (2016).

3.2. Methods

3.2.1. Velocity field and seismic resolution

The generation of a detailed and reliable seismic velocity field is crucial for accurate depth estimation of geological elements (Yilmaz, 2001). We used the conventional velocity analysis of the Echos© industrial seismic software (Fig. S1). The detailed velocity field allowed us to determine sediment layer thickness. Selected seismic lines, identified as crucial for our PQ analysis, were depth converted (Fig. S1b).

Seismic resolution is a fundamental parameter in the interpretation of sedimentary geometries, especially of thin layers (Kallweit and Wood, 1982). By integrating datasets with different resolutions, we were able to identify deep features of different sizes. The PQ sequence, characterized by the maximum frequency range and maximum seismic resolution, shows many thin or small structures that are distinctly visible in the higher resolution WS10 profiles. To emphasize the different resolutions of the profiles used in this study, we compared a WS10 profile with an ES profile. Both cross a shallow, thin sequence with sigmoidal reflectors (c1) and a deeper, thicker sequence of oblique and parallel reflectors (c2) on the continental shelf, at approximately the same location (Fig. S2). Given that the PQ sequence has a velocity range of 1550–2000 m/s, the vertical resolution in the WS10 profiles is estimated to be between 4 and 6 m, based on a dominant frequency of 85 Hz (Fig. S2a). In contrast, the ES profiles, with a dominant frequency of 25–30 Hz, exhibit a vertical resolution of between 13 and 16 m (Fig. S2b).

3.2.2. Seismic Interpretation

The interpretation of seismic lines in the West Sardinian offshore region was conducted using Schlumberger Petrel® software, where horizons, major faults and other geological features were manually picked. As the studied area was affected by magmatic episodes at different ages, we mapped the corresponding evidence using seismic volcano-stratigraphy (Planke et al., 2000; Horni and Geissler, 2014; Horni et al., 2017). Volcanic bodies typically exhibit a conical shape, with high seismic amplitude at their flanks and top, and chaotic medium amplitude internal reflections. Additionally, thin magmatic layers around volcanic edifices are often characterized by continuous high amplitude reflections.

Isochrone maps were generated using the convergent interpolation algorithm, which is effective in maintaining general trends in data-sparse areas, while preserving details where data is available. This method proved optimal for handling the uneven data distribution across the study area. For the Ms isochrone, constraint points for Messinian outcrops alongshore were integrated, based on the onshore geology by Carmignani et al. (2016), to ensure consistency. As with most 2D seismic profiles, the produced maps are strongly influenced by the spacing
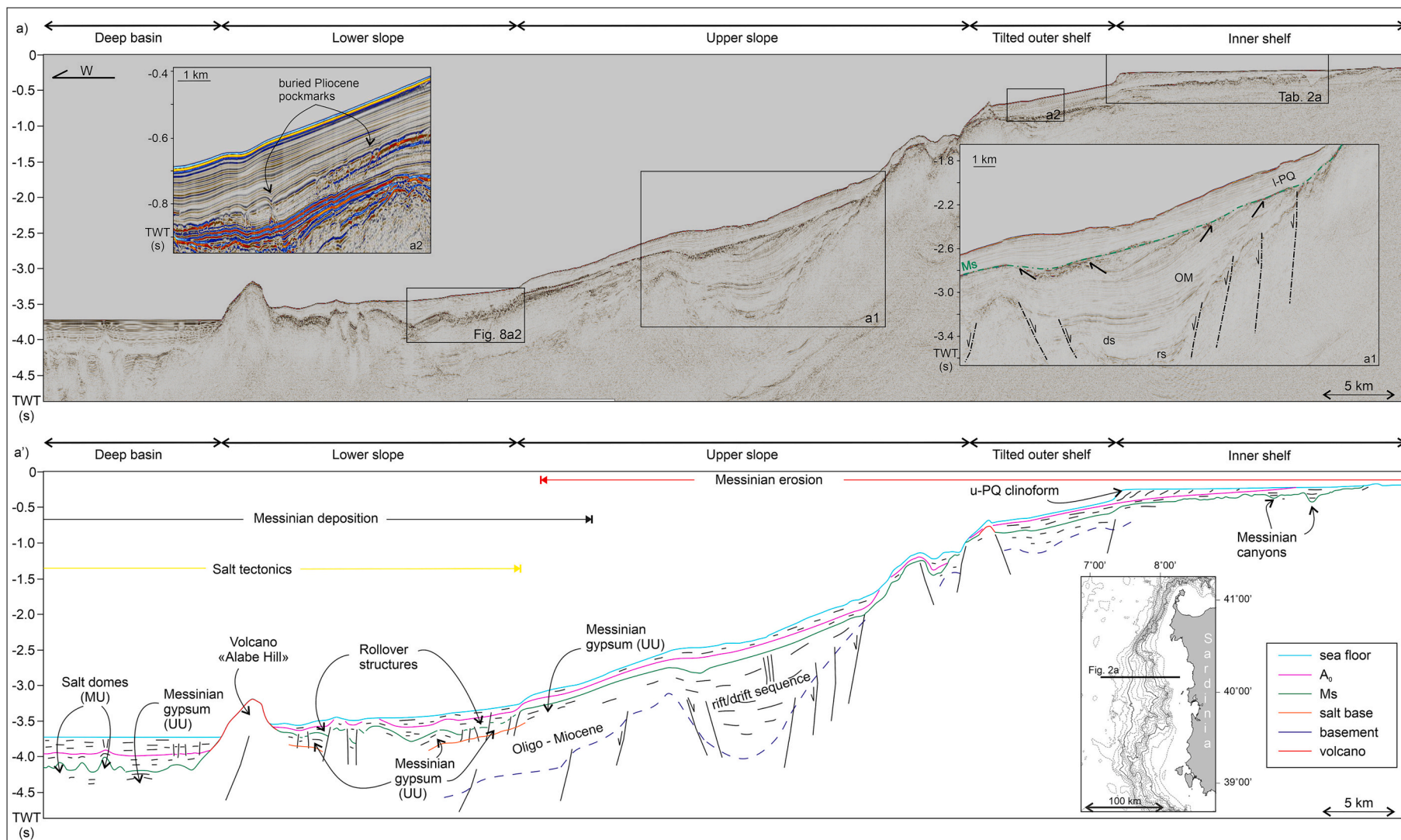
Fig. 2. Uninterpreted seismic profiles WS10–07 (a) and WS10–13 (b) and respective line drawings (a' and b'). The rectangles highlight some of the main features discussed in this paper and in Table 2. Location map of the two seismic transects: bathymetry with dashed lines every 0.2 ms and bold lines every 1 s (TWT). Zoom a1: The chaotic (rs) and more regular (ds) sequences could represent the deposition during the rifting and drifting extensional phase, respectively. Zoom a2: buried Pliocene pockmarks. Zooms b1 and b2: supposed magmatic buildings. Vertical exaggeration: 5.
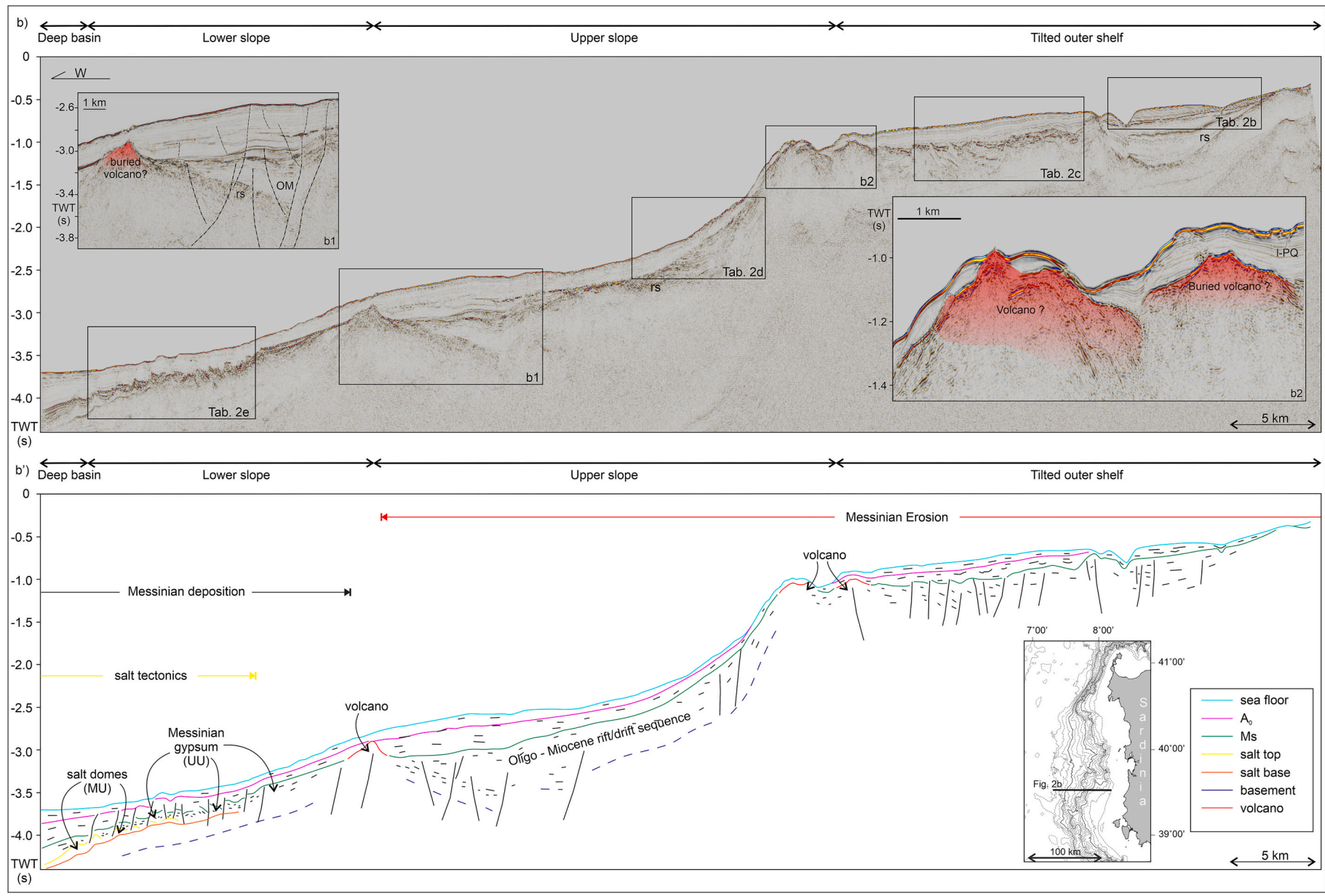
b)

Deep basin | Lower slope | Upper slope | Tilted outer shelf

W

1 km

buried volcano?

rs

OM

b1

TWT (s)

b1

Tab. 2e

Tab. 2d

rs

b2

Tab. 2c

Tab. 2b

rs

TWT (s)

1 km

l-PQ

Volcano ?

Buried volcano ?

b2

5 km

b')

Deep basin | Lower slope | Upper slope | Tilted outer shelf

Messinian Erosion

volcano

Messinian deposition

salt tectonics

volcano

Oligo - Miocene rift/drift sequence

Messinian gypsum (UU)

salt domes (MU)

Sardinia

Fig. 2b

sea floor
A_0
Ms
salt top
salt base
basement
volcano

100 km

5 km

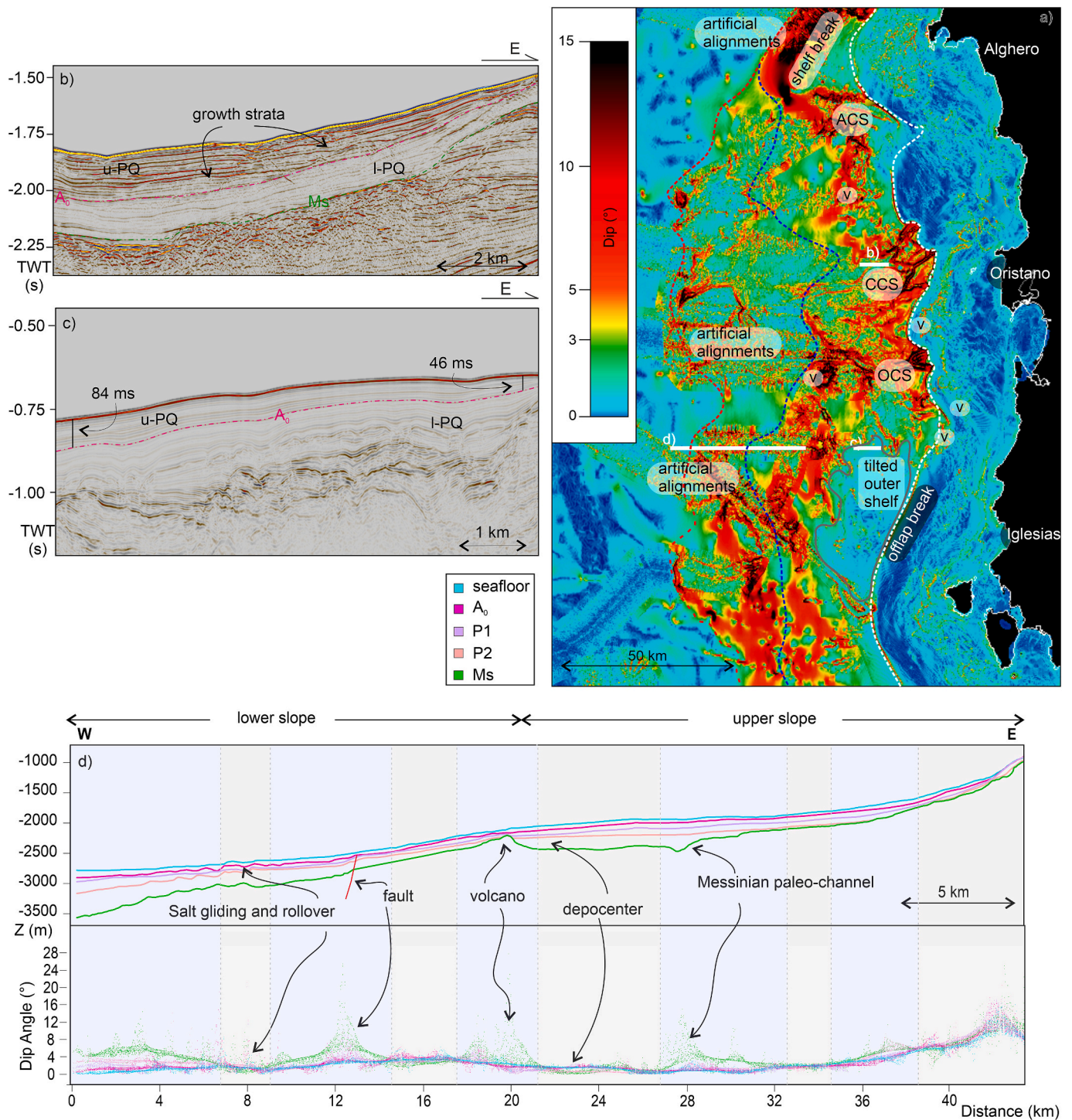TWT (s)

Fig. 2. (*continued*).

Fig. 3. Physiography and dip analysis. a) Dip attribute on the EMODnet (2016) bathymetry. Artificial alignments are due to the position of data acquisition. ACS, CCS and OCS are respectively the Alghero, Il Catalano and Oristano Canyon Systems; V are the outcropping volcanic bodies; the white, blue and red dashed lines represent the offlap break, the transition from upper slope to lower slope, and the base of the slope, respectively. b) Part of the seismic profile WS10–09 in which the l-PQ is more inclined than the u-PQ, suggesting a post-l-PQ increased tilting towards the deep basin. c) Part of the seismic profile WS10–13 showing a different u-PQ thickness on the tilted outer shelf. d) Dip angle distribution of the different reflectors in legend, along part of the seismic profile WS10–13 (Fig. 2b), with the main sedimentary features correlated to the variation of dip of the horizons. (For interpretation of the references to colour in this figure legend, the reader is referred to the web version of this article.)

between profiles. To address this, the bathymetry trend and random points extraction were used to statistically extrapolate and interpolate the distribution of small-scale features, such as salt diapirs, that would otherwise not be imaged (Frisicchio et al., 2023). Isochore maps were obtained as the difference (in TWT) between the shallower and the deeper isochrone maps (e.g. the PQ isochore is obtained subtracting the seafloor isochrone from the Ms isochrone).
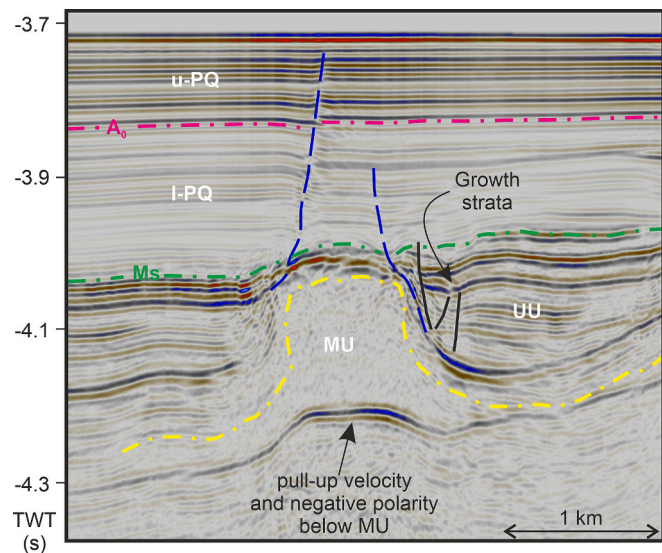
Fig. 4. Seismic facies in the West Sardinian margin. u-PQ = high amplitude upper Plio-Quaternary unit; l-PQ = low amplitude lower Plio-Quaternary unit; UU = Upper Unit and MU = Mobile Unit of the Messinian evaporites. Horizon A_0 separates u-PQ and l-PQ, Ms is the base of the Plio-Quaternary sequence. Growth strata in the UU testify that halokinesis started during the Messinian. Note the negative polarity (blue reflector) and the pull-up effect at the MU base and the typical normal faults above the salt diapir. Vertical exaggeration of WS10–05 (Fig. 1b for location): 5. (For interpretation of the references to colour in this figure legend, the reader is referred to the web version of this article.)

4. Results

4.1. Physiography

The West Sardinian offshore region is divided into three main physiographic provinces: continental shelf, continental slope and deep basin (Figs. 2a, b and 3). The continental shelf is further subdivided into the inner (down to 200 m water depth) and outer (down to 600 m water depth) domains. The inner continental shelf in gentler (Fig. 2a, b) and has a mean gradient of about 0.5°, with local higher values (4–7°) (Fig. 3a). The outer shelf is steeper, with an average gradient of 1° in the Alghero and Oristano area (Figs. 2a, 3a), while it flattens in the Iglesias region (Figs. 2b, 3a). The inner and outer shelf are separated by a narrow (200 m wide), steep (5° gradient) scarp (Fig. 3a). The continental slope is steeper, ranging from 4° to 11°. It can be divided into the upper (down to 2300 m water depth) and lower (down to 2800 m water depth) slopes (Fig. 3a), based on gradient variability. The upper slope shows localized areas of steep inclination, reaching up to 15° where canyon systems are present (Fig. 3a). In contrast, the lower slope (Fig. 2a, b) displays less gradient variation (1° to 5°). The continental slope transitions into the deep basin, which features a predominantly horizontal seafloor (Fig. 3a).

4.2. Seismic stratigraphy

We used specific chronostratigraphic markers (Fig. 4) to constrain the PQ stratigraphy of the West Sardinian margin and adjacent basin: i) Ms boundary (Fig. 5a), representing the base of the lower Plio-Quaternary (l-PQ) deposits; ii) A_0 (Fig. 6a) boundary, marking the base of the upper Plio-Quaternary (u-PQ) deposits, and iii) the present-day seafloor.

The Ms boundary is an erosive irregular surface of high amplitude on the continental shelf and slope, and is concordant in the deep basin (Fig. 2a, b). Ms truncates the pre-Messinian fractured sequence, creating a variable hiatus in the upper pre-Messinian sequence (Figs. 2a1, b; Table 2d) on the upper slope. It bounds the top of the Messinian UU

gypsum on the lower slope and deep basin (Fig. 2a, b). The Ms boundary has a mean dip value of 4.6° (Fig. 3d) and reaches its maximum depth (5.5 s TWT) at the Rhône fan, in the northwestern part of the study area, where it appears undulated and quite irregular (Fig. 5a). To the south, Ms has a depth of about 4.5 s TWT, is smoother with minor irregularities (Fig. 5a). Concerning the A_0 boundary, it is generally a concordant surface, marking the transition from a lower, more transparent seismic facies to an upper, more reflective one. This transition is more evident in the northern part of the basin (Fig. 4). A_0 has a mean dip value of 3.2° and, like Ms, is an irregular surface in the Rhône fan region (Fig. 6a), where it reaches its maximum depth (4.4 s TWT). On the continental shelf, A_0 approximately coincides with the sea bottom (Fig. 6b). In regard of the seafloor, it is commonly a high acoustic amplitude erosive surface and appears irregular towards the Rhône fan (Fig. 1b), where it reaches its maximum depth (4.2 s TWT).

These chronostratigraphic boundaries allow to divide for the first time the PQ sequence into the l-PQ and u-PQ units and to characterize their facies, distribution and thickness.

The l-PQ unit comprises parallel, stratified facies defined by continuous reflections of low amplitude, which increases gradually upwards in the deep basin and more sharply in the continental slope. This unit in commonly relatively thin (130 ms TWT thick) or absent in the continental shelf (Fig. 6c). Here, where present, it is characterized by stratified facies showing horizontal (Fig. 2a; Table 2a), and oblique (Fig. S2) patterns, as well as transparent and chaotic facies (Fig. S3). Locally, the lateral continuity of the l-PQ unit is affected by small depressions (100 m wide, 20 ms TWT deep) (Fig. 2a2, b; Table 2c). On the continental slope, the l-PQ unit is characterized by inclined and parallel reflections, becoming wavy on the lower slope, where wedge shaped strata are also observed (Fig. 2a, b, 7a2; Table 2e). The l-PQ reaches its maximum thickness (1.6 s TWT) in the deep basin, particularly in the Rhône fan region (Fig. 6c), where it also shows the greatest variability. Here, the l-PQ unit is sometimes deformed by the presence of conical structures (up to 1500 m diameter and 500–700 ms TWT in height) (Fig. 2a, b).

The u-PQ unit is distinguished by high amplitude, well-stratified and continuous reflections (Fig. 4). It is generally absent or relatively thin (150 ms TWT) on the continental shelf and slope (Fig. 6b). Where present on the shelf, the strata configuration is characterized by a wedge shape geometry that is internally defined by sigmoidal reflections (Fig. 2a; Table 2a), downlapping onto the A_0 or Ms boundaries (Figs. 2a, b, 3c; Table 2a, c). On the continental slope, the u-PQ unit shows parallel reflections, which are sometimes inclined and wavy (Fig. 2a, b). The u-PQ thickness increases sharply in the deep basin (up to 1.0 s TWT), particularly towards the Rhône fan region (Fig. 6b), although it shows less variability than the l-PQ (Fig. 6c). In this physiographic domain, the u-PQ reflections are mostly horizontal and parallel, and locally wavy or slightly inclined (Figs. 2a, 4).

4.3. Significant geological structures and features affecting the Pliocene and Quaternary units

Different significant geological structures and features affect the Pliocene and Quaternary units characterizing the West Sardinian continental margin and adjacent basin. They are the following: a) salt tectonic structures, b) normal faults, c) magmatic volcanoes, d) pockmarks, e) canyon systems and canyon fill deposits and e) regressive clinoform system.

4.3.1. Salt tectonic structures

This type of structures plays a prominent role in deforming the entire PQ sequence, both in the lower continental slope (Fig. 2b; Table 2e) and adjacent deep basin (Fig. 4; Table 2f). These structures primarily consist of diapirs, which can reach up to 1.5 km in width and 700 ms TWT in height. The diapirs are rooted in the Messinian sequence and penetrate both the lower and upper PQ units (pink area in Fig. 7), leading to
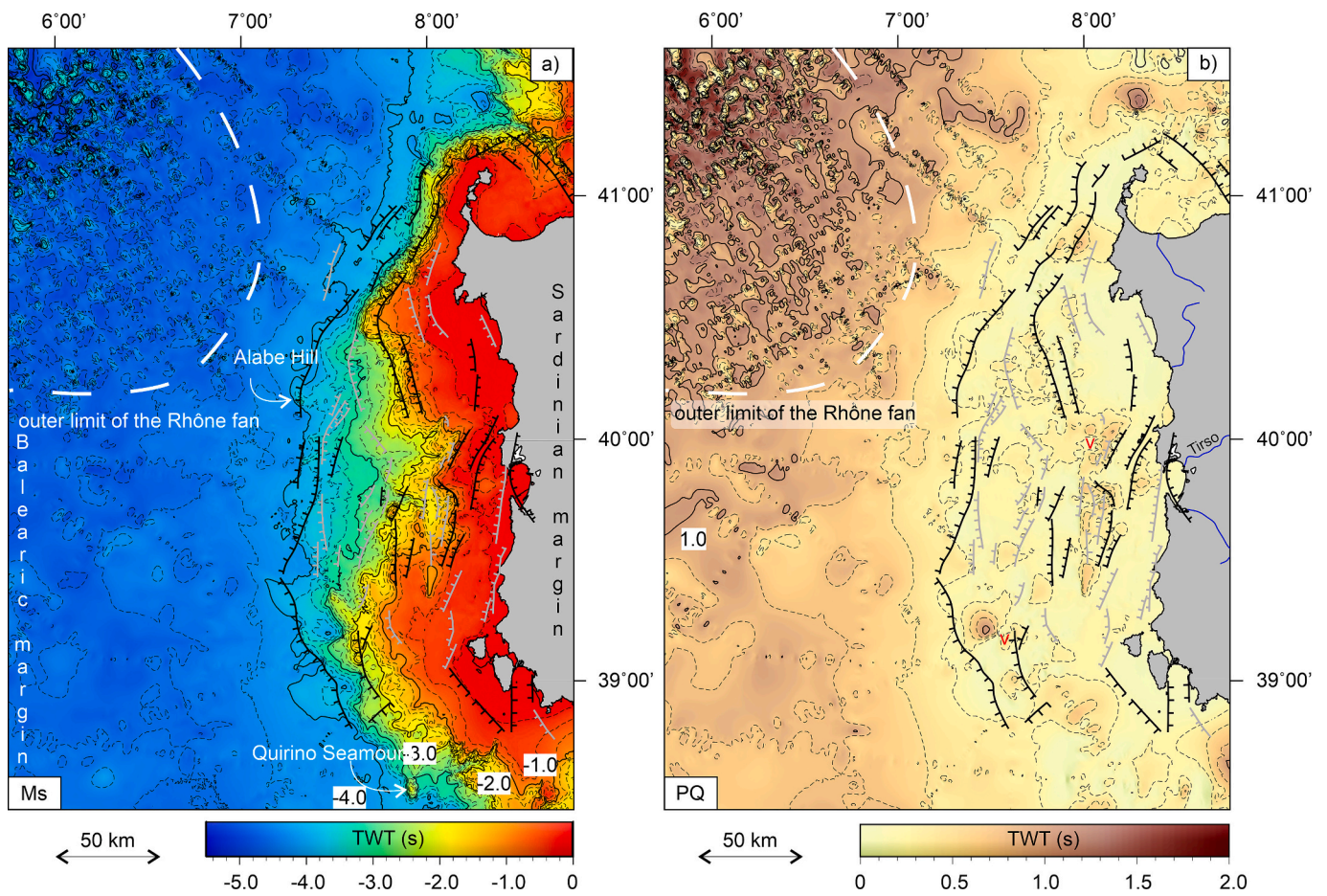
Fig. 5. a) Isochrone map of the Ms reflector/PQ base; b) Isochore map of the PQ thickness, v are volcanoes; see the text for comments. PQ faults are in black, OM faults in grey in both panels. The outer limit of the Rhône fan deposits is the white dashed line. In blue the main rivers onshore Sardinia. Dashed contour lines every 0.25 s TWT, bold lines every 1.0 s TWT. (For interpretation of the references to colour in this figure legend, the reader is referred to the web version of this article.)
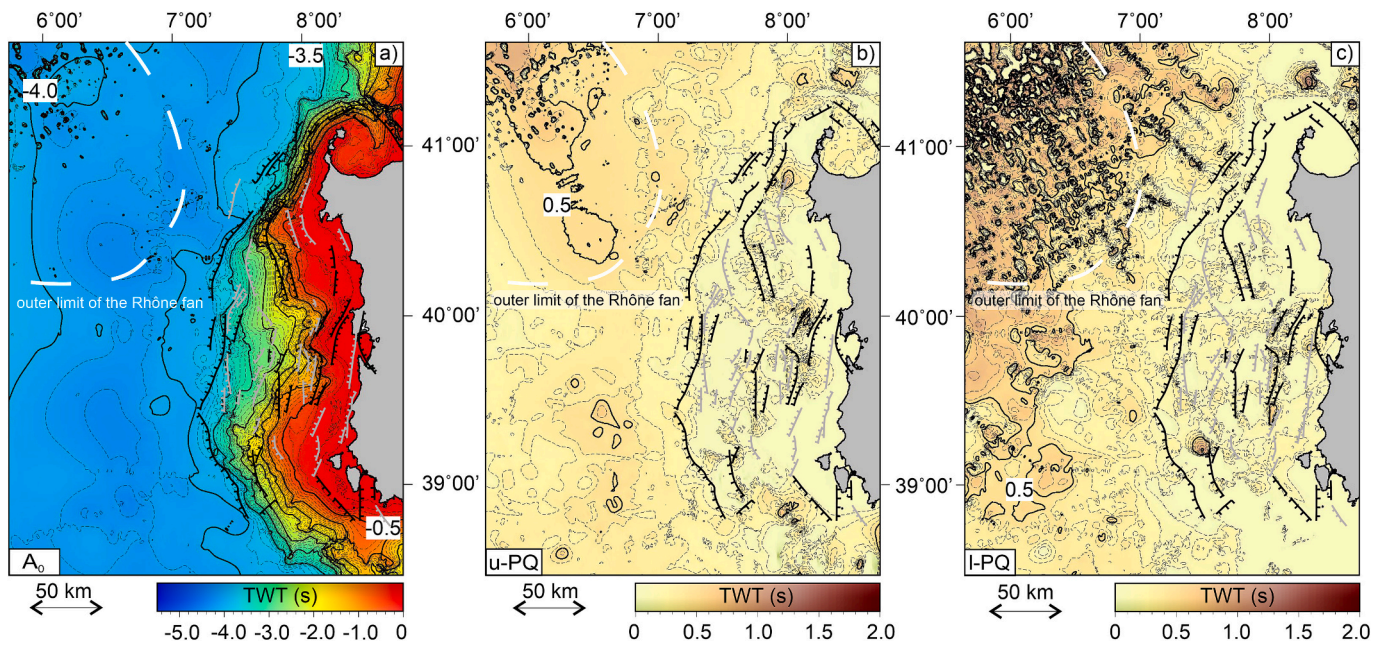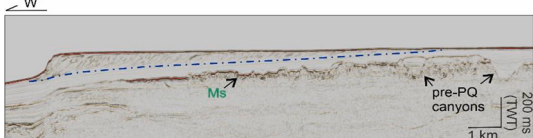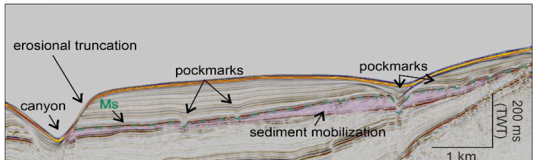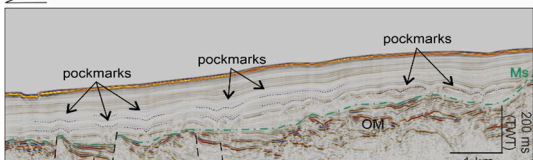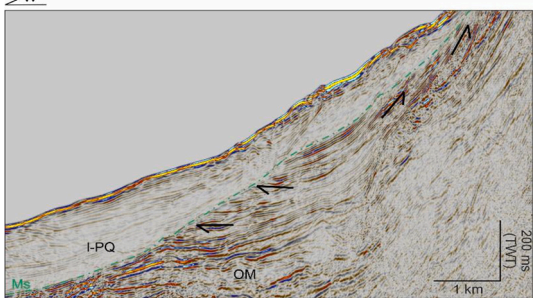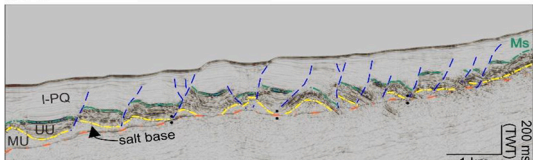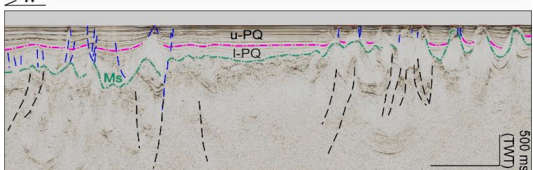

Fig. 6. a) Isochrone map of reflector A_0, only based on available seismic profiles; b) u-PQ isochore; c) l-PQ isochore; the northwestern part of maps in b) and c) are better defined thanks to the integration with data from Bellucci et al. (2021b); PQ faults are in black, OM faults in grey in both panels. The outer limit of the Rhône fan deposits is the white dashed line. Dashed contour lines every 0.1 s TWT, bold lines every 0.5 s TWT.

Table 2

Description of the main features of the West Sardinian margin on WS10 profiles. a) to e) location on Fig. 2a and b; f) location on Fig. 1b. The pre-Pliocene sequence is assumed to be Oligo-Miocene (OM) in age.

Features	Description	Seismic
a) clinoform	Clinoforms are the shallowest deposits enlarging the inner continental shelf. Note the Messinian canyon completely filled by the PQ sequence.	
b) Sediment mobilization and pockmarks	The mobilized unit, located on the continental shelf, is characterized by low amplitude chaotic reflections. Pockmarks deform Ms and some of the lower Pliocene reflectors: these features are associated with the release of gas or fluids.	
c) Faulted pre-Pliocene sequence and pockmarks	The pre-Pliocene sequence (OM) is characterized by normal faulting, creating a horst and half-graben structure. Ms erodes part of the OM sequence. The lower part of the PQ sequence is characterized by growth strata and pockmarks that do not reach the seafloor.	
d) Messinian Erosional Surface	On the shelf and upper slope, Ms is a high amplitude, erosive horizon, recognizable by the onlap termination of the overlying strata and the erosional truncation of the pre-Pliocene (OM) sequence. Since it is the only Messinian element on the shelf and upper slope, the Plio-Quaternary sequence lies directly above the OM megasequence.	
e) Rollover structures	The lower slope is characterized by a system of rollover structures that affect the Messinian sequence: normal faults cut the Mobile Unit (MU), the Upper Unit (UU) and most of the PQ sequence, where we can identify growth strata. The base of the PQ conformably lies above the UU and no evidence of erosion are present.	
f) Halokinesis effects	Halokinesis affects the PQ sequence producing thickness variability and numerous faults (in blue). The black faults are pre-Pliocene, generally related to the OM extensional phase.	

undulated and wavy configurations in the strata pattern. The salt related deformation is evidenced by rotated UU and l-PQ blocks (Figs. 2b, 8a2; Table 2e), bounded by rollover associated faults that modify the geometry of the Ms boundary (Fig. 3d). These faults flatten downward and converge with the Messinian salt base (Table 2e). They also cut through the PQ sequence, reaching and deforming the seafloor (Table 2e), where they create undulations and small depressions (30–40 ms TWT). In addition, typical crestal conjugate normal faults (Fig. 8c) form above diapiric structures in the deep basin. These crestal faults converge downward at the top of the salt diapir and cut the overlying l-PQ and u-PQ units, locally reaching the seafloor (Fig. 8c), where they produce small scarps (15–20 ms TWT).

4.3.2. Normal faults

These faults have subvertical planes and affect l-PQ and u-PQ units mostly in the continental slope (Figs. 2b, 9a; Table 2c, d) and shelf (Figs. 3a and 9b, c, d, e). They extend downward offsetting the Messinian sequence (green colored lines in Fig. 7), where other similar faults are imaged (brown colored lines in Fig. 7) and form horst-and-grabens filled and covered by the chaotic OM sequence (Fig. 2a1). PQ sediments affected by normal faults appear tilted, locally wedge shaped, in particular the l-PQ unit (Fig. 9a). The u-PQ unit is locally affected by the normal faults (Fig. 2b1), with smaller displacements (15 ms TWT). North of the Gulf of Oristano, normal faults abruptly cut the seafloor (Fig. 9b, d, e), generating block tilting that has favored the outcropping
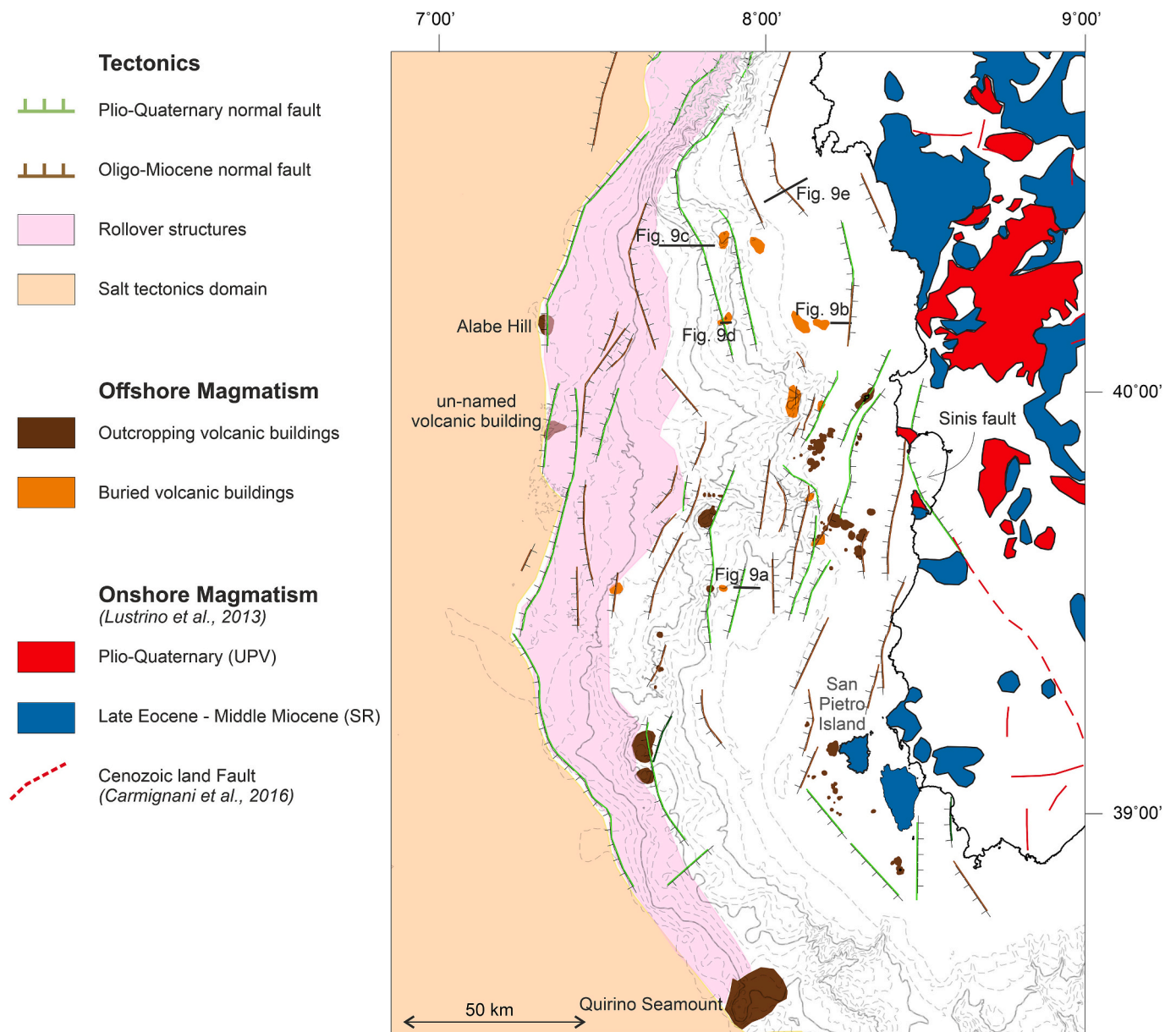
Fig. 7. New structural map of the West Sardinian margin. Fault systems in the West Sardinian margin interpreted in this work and partially recovered by literature (Torelli et al., 1990; Bigi et al., 1992a, 1992b; Fais et al., 1996; Faccenna et al., 2002; Sage et al., 2005; Oudet et al., 2010), integrated with the volcanic buildings. The Sinis Fault delimits the Gulf of Oristano and the Campidano Graben, acting like a threshold separating them from the western Sardinian shelf (De Falco et al., 2022). Bathymetric contour lines are every 0.25 s TWT, bold every 1 s TWT (corresponding to 750 m). In the onshore area, the two main magmatic phases are taken from Lustrino et al., 2013: UPV (Unradiogenic Pb Volcanic) and SR (subduction-related).

of pre-Messinian layers and the development of microfractures (Fig. 9c2). These features at the seafloor create scarps (150 ms TWT depth) and sub-rounded depressions (140 ms TWT relief, 500–1500 m width).

4.3.3. Magmatic structures

Magmatic structures (volcanoes) are prominent features along the West Sardinian margin, with both buried and outcropping edifices that are located above the Ms boundary, particularly in the CVF area (Fig. S3a), and are onlapped by u-PQ reflections (Figs. 2b1, b2, 9d). These structures are characterized by conical cross sections, internally defined by chaotic and transparent seismic facies (Fig. S3a), and display circular shapes in plan view (Fig. 7). Based on their dimension, small, medium and large volcanoes are identified. Small volcanoes measure 100–200 m in diameter and 40–120 ms TWT in height, with a medium

peak elevation of 110 m and basal depth of 170 m. They cut through the PQ sequence and outcrop on the continental shelf, showing truncation at their peaks (Fig. S3a and b). Medium volcanoes, measuring approximately 1.5 km in diameter and 200–300 ms TWT in height, penetrate the l-PQ sequence and only locally a few reach the seafloor (Fig. 2b1, b2). Finally, three large volcanoes, with approximately 3 km diameters and height up to 500 ms TWT, are located at the transition between the continental slope and deep basin (Figs. 2a, 7 and S3c, d). These include: the Alabe Hill (Fig. 2), an unnamed structural high (Fig. S3d), and the Quirino Seamount (Fig. S3c), with peak elevations of 2390 m, 2320 m, and 1880 m, and basal depths of 2750 m, 2600 m and 2140 m, respectively. They are all onlapped by the pre-Pliocene sequence, and among these, only the Quirino Seamount has been sampled, confirming its magmatic lithology dating to the OM period (Lecca, 2000).
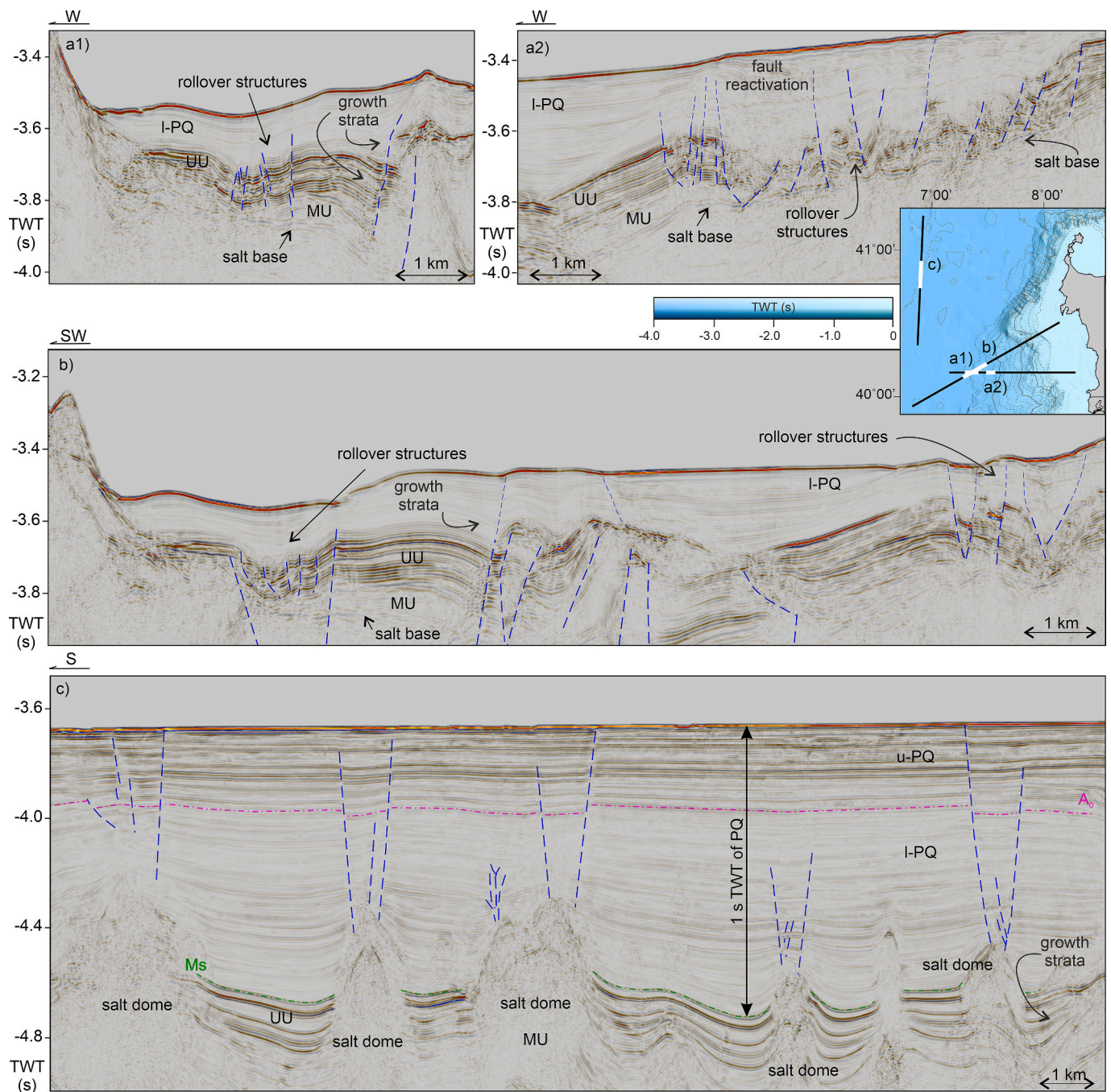
10

Fig. 8. Effects of salt tectonics in the lower slope (a1, a2, b) and in the deep basin (c), where the PQ reaches a thickness of 1 s TWT, corresponding to approximately 1 km. Vertical exaggeration: 5. a) Segments of the seismic line WS10–07; b) part of the seismic line WS10–02; c) part of the seismic line WS10–04.

4.3.4. Pockmarks

Pockmarks, ranging from 80 to 200 m in diameter, disrupt the lateral continuity of the l-PQ and u-PQ deposits on the outer continental shelf. These features typically display a V- shaped cross section that transitions to a U-shape upwards (Figs. 2a, b, and S4). Pockmark seem to occur above normal faults cutting both the pre-Pliocene and the PQ sequence (Fig. 2a2, b; Table 2c) and appear vertically stacked, some of them reaching the seafloor (Fig. S4a, b) and exhibiting a predominant NW-SE orientation (Fig. S4a). Seafloor pockmarks are also mapped aligned along a N-S valley extending into the Oristano Canyon System (Figs. 10 and S4a).

4.3.5. Canyon systems and canyon fill deposits

Three canyon systems with predominantly straight and rarely sinuous trends have been recognized incising orthogonally the northern sector of the West Sardinian margin and west of the Gulf of Oristano. These systems follow N*E*-SW and E-W orientations (Fig. 10) and have been named, from north to south, as Alghero (ACS), Il Catalano (CCS) and Oristano (OCS). Branches a and c of the CCS were previously identified by Ulzega (1988) as "Mannu Canyon" and "Putzu Idu", while branches c and d of the Alghero Canyon System were collectively termed the Logudoro Canyon by Ulzega (1988). These canyon systems, classified as shelf-incising, range from a few hundred meters to several kilometers in width, particularly in their lower course, and from tens to a few hundred meters in depth, especially in their upper course (Fig. 10).
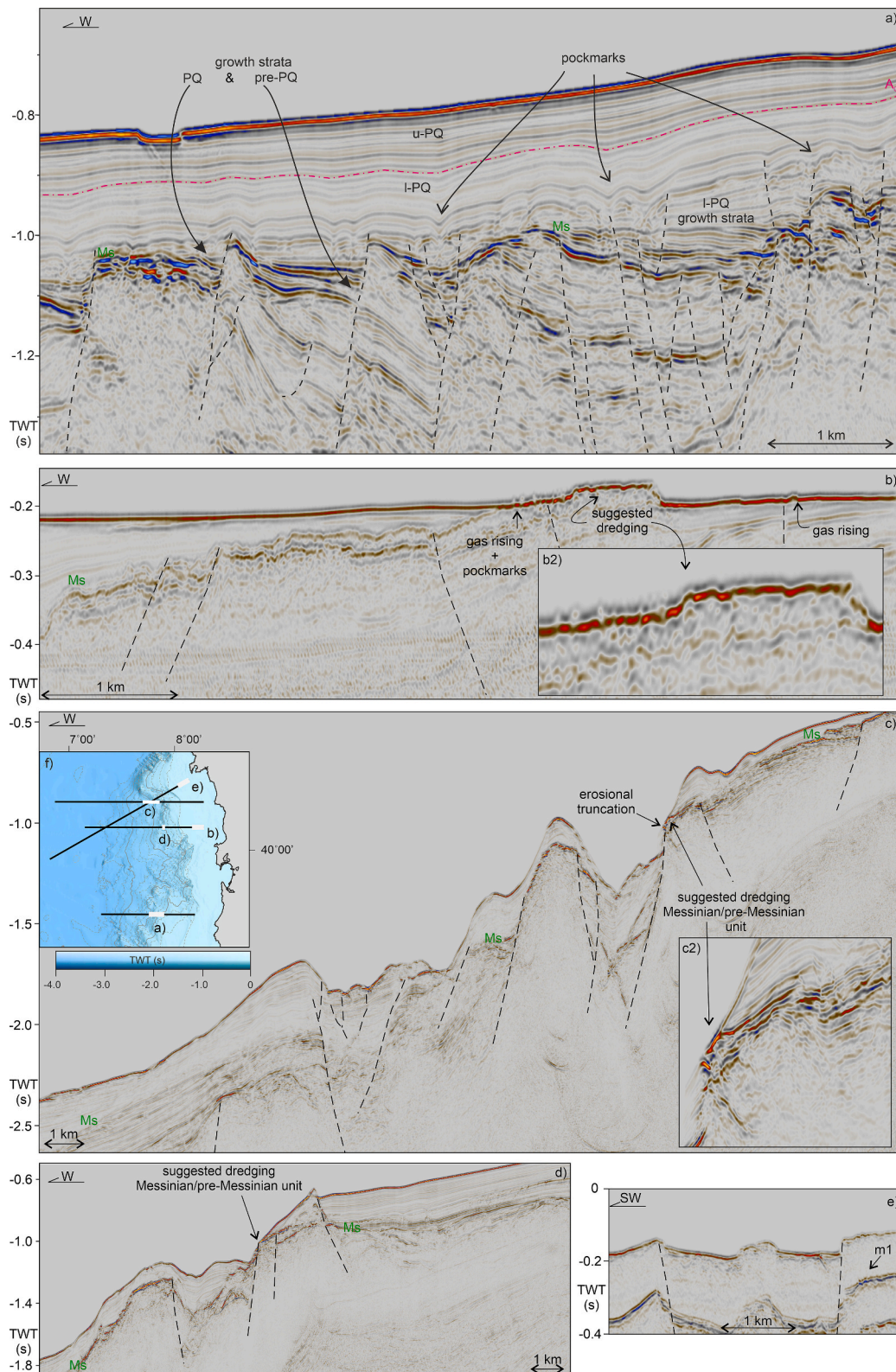
Fig. 9. Examples of PQ normal faults in the West Sardinian margin. a) Part of the seismic line WS10–13: l-PQ unit shows wavy reflectors and buried pockmarks related to gas rising through normal faults and mobilizing the sediments; b) part of the seismic line WS10–07: blocks rotation cause outcrops of a pre-Pliocene sequence of unknown lithology with evidence of gas seeps; c) part of the seismic line WS10–05: some sedimentary mounds originated during the last depositional event, several faults cut Ms and the PQ sequence, often reaching the sea bottom and sometimes causing the outcropping of the pre-Pliocene sequence (sites of suggested dredging); d) part of the seismic line WS10–07: faults cutting Ms and the PQ sequence, sometimes causing the outcropping of the pre-Pliocene sequence (sites of suggested dredging); e) part of the seismic line WS10–02: two faults cut the sea bottom where the pre-Pliocene sequence outcrops, m1 is the first multiple. Vertical exaggeration 5.
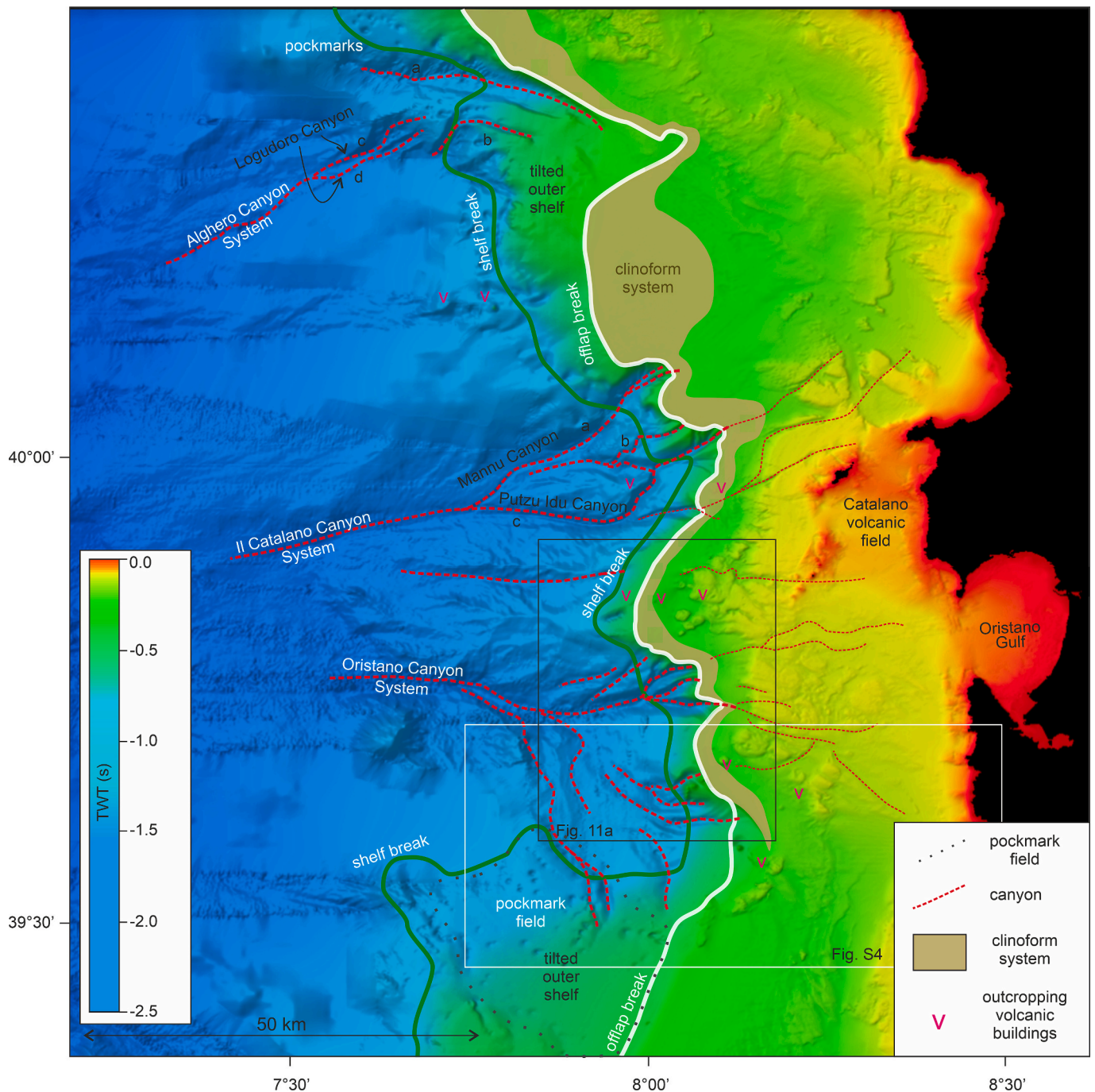
Fig. 10. Main features of the seabed, identified on the bathymetry and through seismic interpretation.

Generally, they erode the subparallel u-PQ layers, and in some cases, sedimentary deposits on both sides of the canyons dip towards the thalweg on the outer shelf, as evident for the OCS (Fig. 11b). On the continental shelf, the canyons are infilled with PQ sediments, obliterating totally or partially their seafloor bathymetric expression (Fig. 11a). A few canyons from the OCS erode reaching the Ms boundary. The sedimentary fill, which typically exhibits a triangular cross-shape section, consistently shows high amplitude reflections in the thalweg, which are occasionally chaotic and sometimes U-shaped (Fig. 11b, d).

4.3.6. Regressive clinoform system

Seaward downlapping regressive deposits with progradational sigmoidal reflections build a recent shelf clinoform system, 40 ms to 140 ms TWT thick and approximately 100 km long (Fig. 10). An offlap break

creates the narrow steep scarp mapped at the seafloor and that separates the inner and the outer continental shelf. The clinoforms downlap the l-PQ parallel (Fig. 2a; Table 2a) or wavy layers (Fig. 12b, c), or the older Pliocene oblique reflections (Fig. 12b). In the northern sector, between the Alghero and Oristano canyons (Fig. 10), the regressive clinoform system reaches its maximum width (12 km) and thickness (140 ms) (Fig. 2a; Table 2a). Here, the offlap break is characterized by higher (10°-12°) slope values (Fig. 3a) and is associated with a chaotic unit (Fig. 12a) at the base of the clinoform system. Southward, in front of the Gulf of Oristano, the clinoform system is narrower (2 km) and thinner (40 ms TWT), ending before it reaches the tilted outer shelf (Fig. 10). Analysis of the dip values, obtained through the "local structural dip" attribute applied on a depth converted seismic line (Fig. 12a1), reveals a gradual landward increase in the dip of the foresets. In the northernmost
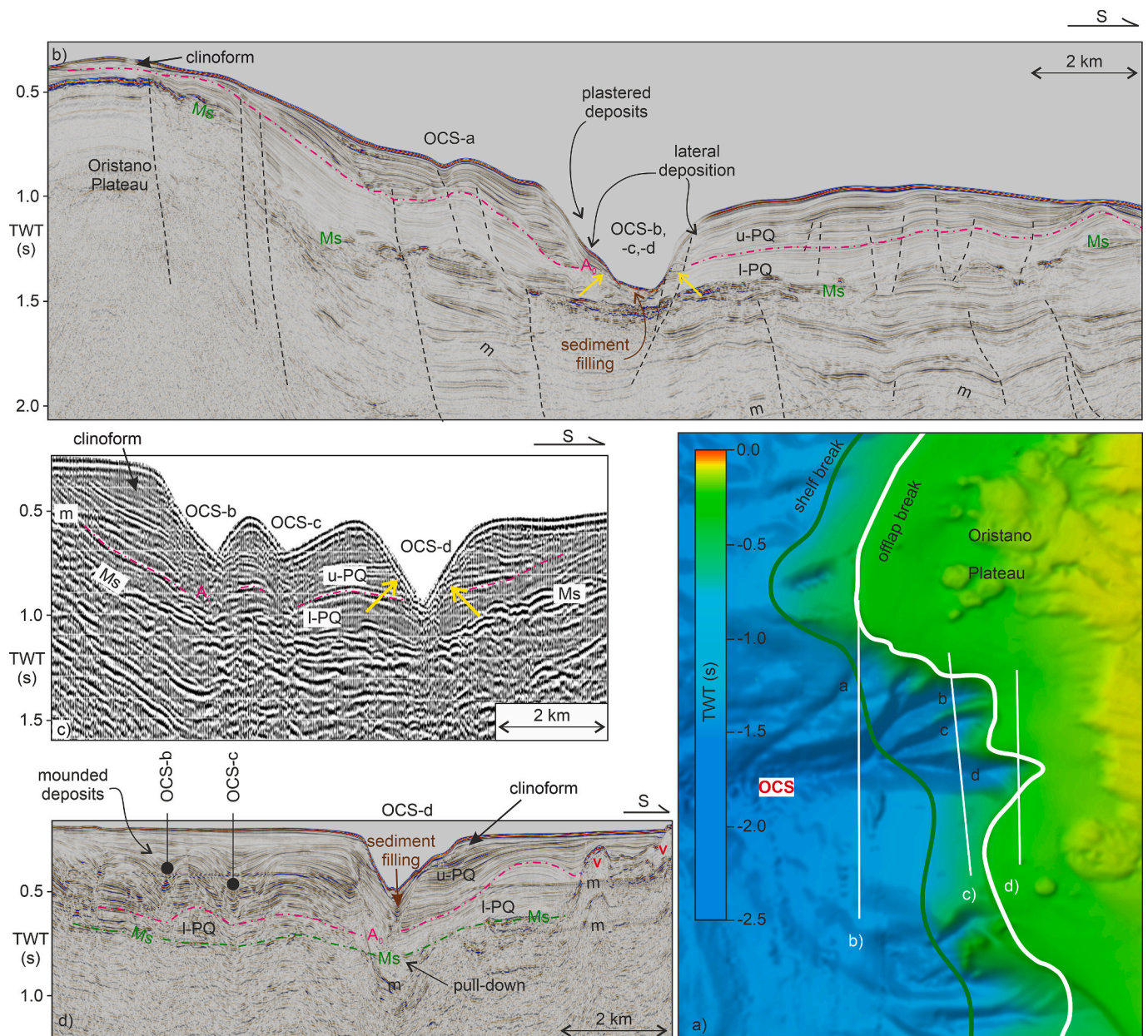
Fig. 11. Details of profiles showing the Oristano Canyon System (OCS). The OCS-b, -c and -d branches show erosional truncation (yellow arrows) on both sides of the canyons. a) location map. (b) Part of the seismic line WS10–14: the northern side of the convergence OCS-b, -c and -d branches, is covered by onlapping and plastered deposits; c) part of the seismic line ES-127: the three branches are separated; d) part of the seismic line WS10–10B: only the OCS-d branch is currently active, while -b and -c are filled and covered by PQ mounded deposits. "v" is for buried or outcropping structures interpreted as volcanoes; "m" is for multiples. Vertical exaggeration: 5. (For interpretation of the references to colour in this figure legend, the reader is referred to the web version of this article.)

area, the clinoform system directly overlies the Ms (Fig. 12a) whereas further south, it downlaps (Figs. S2, 2a and 12b, c, d; Table 2a) onto the eroded top of the underlying PQ sequence.

5. Discussion

During the PQ, several factors contributed to shaping the current structure of the West Sardinian margin and the adjacent Sardo-Provençal deep basin. Here we discuss the different processes and events that influenced the margin and basin development and their mutual relationships (summarized in Fig. 13). We focus on the tectono-sedimentary processes affecting the margin and adjacent basin (Fig. 14), starting from concepts introduced by Fais et al. (1996), Sage et al. (2005), Geletti et al. (2014). While these studies primarily focused

on the opening of the Sardo-Provençal basin and the MSC, they provided limited insight into the PQ evolution of the study area, which this analysis aims to address.

5.1. Stratigraphic age model

Our interpretation of seismic data, particularly the A_0 reflector, provides key insights into the timing of the processes shaping the West Sardinian margin and adjacent basin. The A_0 reflector, identified across the study area, is correlated with the P11 reflector from Leroux et al. (2017) through the intersection of the ECORS profile with our dataset (Fig. 1) and the similarity in seismic facies. Since the P11 reflector is constrained as the base of the Quaternary (ca. 2.6 Ma), in accordance with the revised chronology by the International Commission on
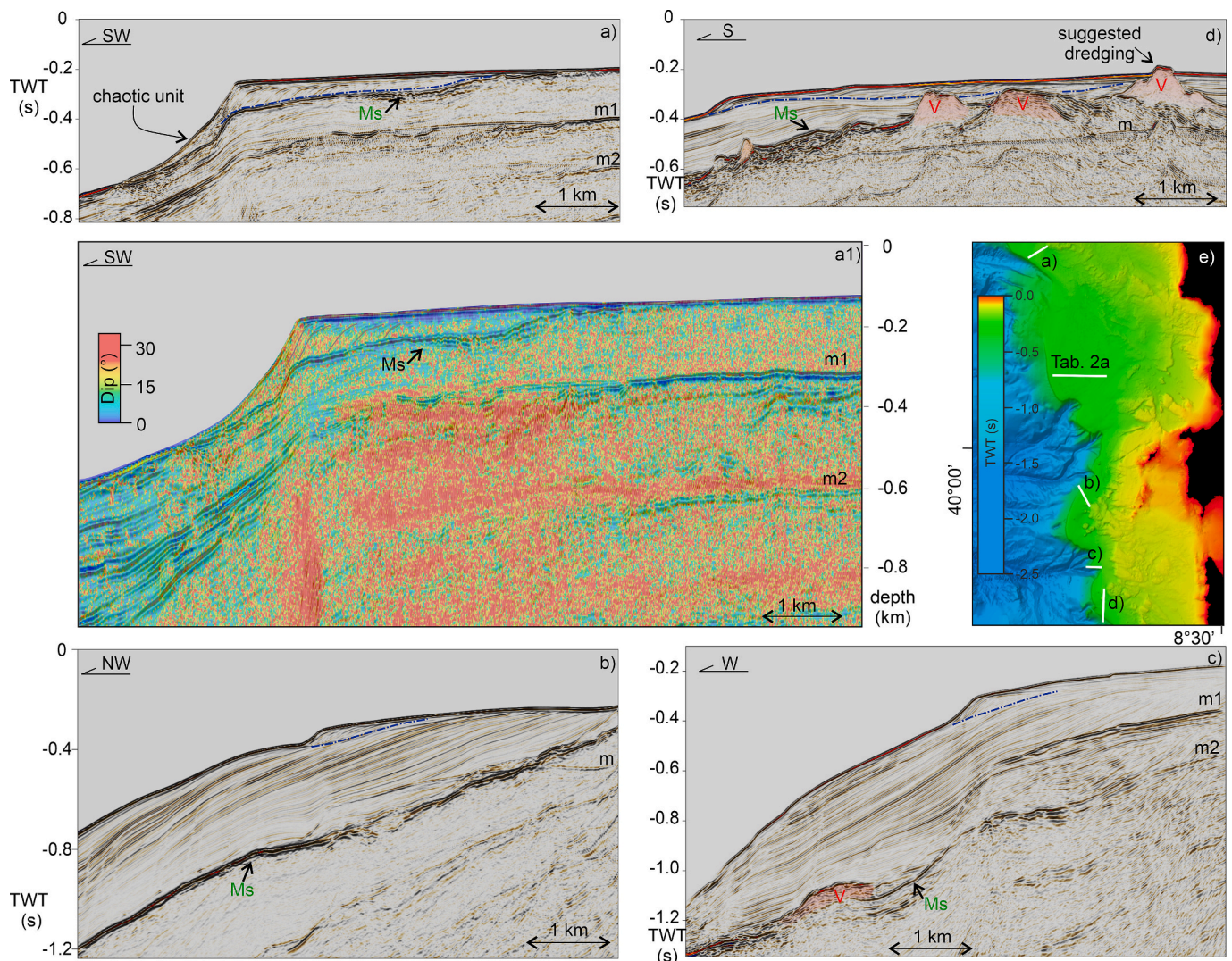
Fig. 12. Clinoform systems of the West Sardinian margin. The blue horizon represents the base of the recent clinoform system, the red areas represent the volcanic buildings (v). a1) local structural dip attribute of the depth-converted seismic line of panel a). Location of the profiles is defined in the bathymetric map e); the width of the recent clinoform system has been depicted in Fig. 10, westward bounded by the offlap break; in d) the outcropping volcano could be easily dredged to furnish the age of this magmatic event. Vertical exaggeration: 5. a) Part of the seismic line WS10–02; b) part of the seismic line WS10–15; c) part of the seismic line WS10–11; d) part of the seismic line WS10–10B. (For interpretation of the references to colour in this figure legend, the reader is referred to the web version of this article.)

Stratigraphy (Mascarelli, 2009), the A_0 reflector can be hypothesized to date back to the same age, coinciding with the intensification of the Northern Hemisphere Glaciations, marked by a major sea level fall (Haq et al., 1987). Based on this interpretation, we infer that the l-PQ and u-PQ units correspond to Pliocene and Quaternary deposits, respectively. The subdivision of the PQ sequence into the Pliocene and Quaternary units, each with distinct seismic facies, has been commonly carried out across various regions of the Mediterranean Sea, such as the Tyrrhenian Sea (Selli and Fabbri, 1971), Sicily Channel (e.g. Civile et al., 2014), Ionian Sea (e.g. Volpi et al., 2017) and Adriatic Sea (e.g. Špelić et al., 2021). In the Alboran Sea, a similar reflector, known as BDQ, has been interpreted as the base of the Quaternary (Juan et al., 2016). However, previous works lacked precise age constraining for the A_0 reflector. Our research aims to offer additional insights that enhance the understanding of the Pliocene and Quaternary depositional and tectonic history of the West Sardinian margin.

5.2. Characterizing vertical movements

Vertical movements of the West Sardinian margin are intricately linked to the regional subsidence and uplift trends. Key factors for the occurrence of both movements include the interplay between thermal subsidence, associated to the OM opening of the basin (Rehaut, 1981; Savoye and Piper, 1991) and the effects of water and sediment loading, ongoing since the MSC (Heida et al., 2022). The westward tilting of the margin is evidenced by the increasing dip of older horizons (highlighted in blue in Fig. 3d) and the westward-thickening growth strata within the PQ sequence (Figs. 3b, c and 9a). The MSC, marked by a dramatic drop in Mediterranean Sea levels (Haq et al., 1987), triggered both erosion and deposition in the region. This sea-level drawdown produced lithosphere unloading, which in turn caused uplift in the basins and their continental margins while subsidence occurred onshore (Norman and Chase, 1986; Gargani, 2004; Roveri et al., 2014). Lower evaporite deposition further influenced vertical movements, potentially leading to significant slope angle changes (Govers et al., 2009; Garcia-Castellanos and Villaseñor, 2011; Roveri et al., 2014). The loading of evaporites, followed by further loading of seawater and sediments after the Zanclean reflooding, partially counterbalanced the earlier unloading related to a thinner water column and to the eroded sediments on the West Sardinian margin. This intensified subsidence and contributed to
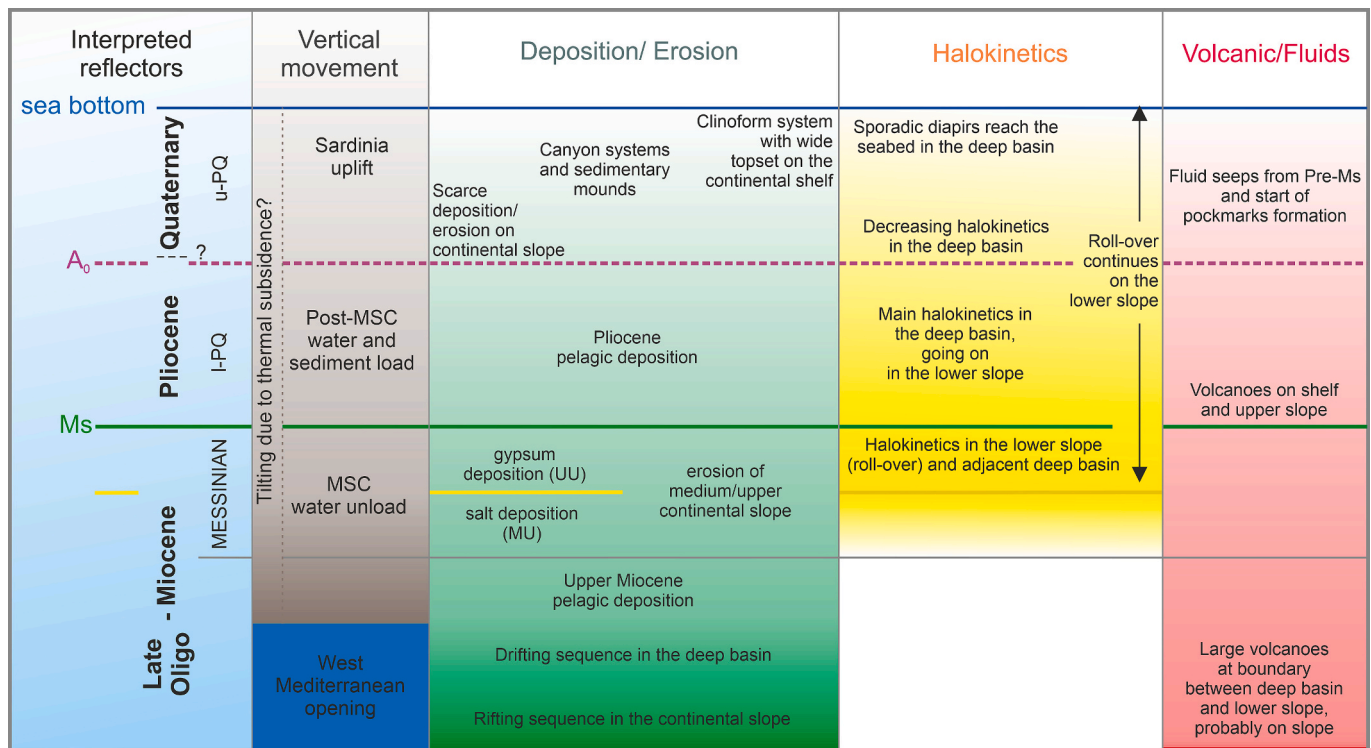
Fig. 13. Summary of the main events that characterize the West Sardinian offshore.

ongoing tilting and fault reactivation of the margin (Brun and Fort, 2011). Furthermore, the continental uplift due to isostatic rebound likely intensified erosion through a feedback process (Gargani et al., 2010). Evidence of Pleistocene uplift in the Sinis Peninsula (Barca et al., 2016; Cocco et al., 2019) and late Miocene marine deposits at 650 m above sea level in Capo S. Marco (Funedda et al., 2012; Coltorti et al., 2015) further support the hypothesis of regional tilting. In the northern Campidano region, Cocco (2013) suggests an uplift of several hundred meters, related to a lithospheric structure originating from the pre-Pliocene evolution of the western Mediterranean. The tilting of the West Sardinian continental margin is closely linked to the reactivation of the OM inherited faults on the continental shelf (Fig. 9b) and upper slope (Fig. 9c, d). Some of these faults extend to the seafloor, favoring local outcropping of pre-Messinian layers, which offer excellent opportunities for dredging the pre-PQ sediments for dating purposes (detail of Fig. 9c2). Recent faults separate the inner continental shelf from the tilted outer shelf blocks. This activity appears to be of Quaternary age, as indicated by the high amplitude west-ward thickening Quaternary growth strata (Figs. 2a2 and 9a).

5.3. Magmatic activity

The West Sardinian margin exhibits significant volcanic activity that took place in two main phases (a single pulse in OM and two pulses during the PQ), as defined by Lustrino et al. (2007a, 2007b). The coincidence of Ms with the base of the volcanoes (Fig. S3a), here characterized in the continental shelf and slope, is consistent with one of the events that took place during the early Pliocene, mostly in the area off the Gulf of Oristano (Lustrino et al., 2007a, 2007b; Geletti et al., 2014; Conforti et al., 2016). In contrast, the magmatic structures surrounding the San Pietro Island (SW of Sardinia) are dated to the middle-upper Miocene (Deiana et al., 2021). The volcanic structure mapped at the boundary between the continental slope and deep basin seem to be older. The Quirino Seamount (Figs. 7, S3) (Finetti and Morelli, 1974) is dated to the OM period (Lecca, 2000). The Alabe Hill (Fig. 7) has never been dated (Geletti et al., 2014; Würtz and Rovere, 2015), although its

physiographic location and the onlapping terminations of the PQ and pre-Pliocene layers suggest that it formed during the OM oceanic opening of the Western Mediterranean. A similar stratigraphic pattern is observed in other volcanoes emerging at the slope-basin boundary (Figs. 2a, 7, S3c, d), suggesting a similar origin. The OM faults, related to the extensional domain of the basin opening, are often interpreted as conduits for magma uplift, leading to the formation of these volcanoes (Peterson et al., 2020).

5.4. Salt tectonics and fluid dynamics

Salt tectonics played a crucial role in shaping the lower slope of the West Sardinian margin and adjacent deep basin. Following the Messinian Salinity Crisis (MSC), the increased load from water and sediment (Fig. 14b) likely enhanced subsidence, driving halokinetic processes primarily through salt gliding (Dos Reis et al., 2005; Brun and Mauduit, 2008; Gaullier et al., 2007; Brun and Fort, 2011; Bellucci et al., 2021a). These processes started during the upper Messinian, as testified by growth strata in the UU (Fig 8a1, b), and intensified during the Pliocene (Fig. 2b, 6c, 8, 14a, b; Table 2f). Rollover structures in the lower slope (Figs. 2b, 8a1, a2, b; Table 2e), and salt diapirs in the deep basin (Figs. 4 and 8c), deformed both the Pliocene and Quaternary units, causing variations in thickness and the formation of localized depocenters, particularly towards the Gulf of Lion. Here, halokinetic tectonics (Figs. 5 and 6), was favored both by the increase of the sedimentary load (Fig. 5b), due to the large amounts of sediments from the major French rivers, and by a thickest salt unit in the central part of the basin, as already suggested by Geletti et al. (2014). This larger amount of salt, also reconstructed by Bellucci et al. (2024), probably originated from a deeper seafloor in the central part of the basin during the Messinian, with additional salt sliding there from the two opposite sides of the basin. The tilted blocks of the roll-over structures are separated by local normal faults (pink area in Fig. 7) that generally follow the flanks of the diapirs and often terminate downward at welds. We suggest that the halokinetic process, originated by the gravity sliding effect due to the downward sloping salt base, has been accentuated by the subsidence
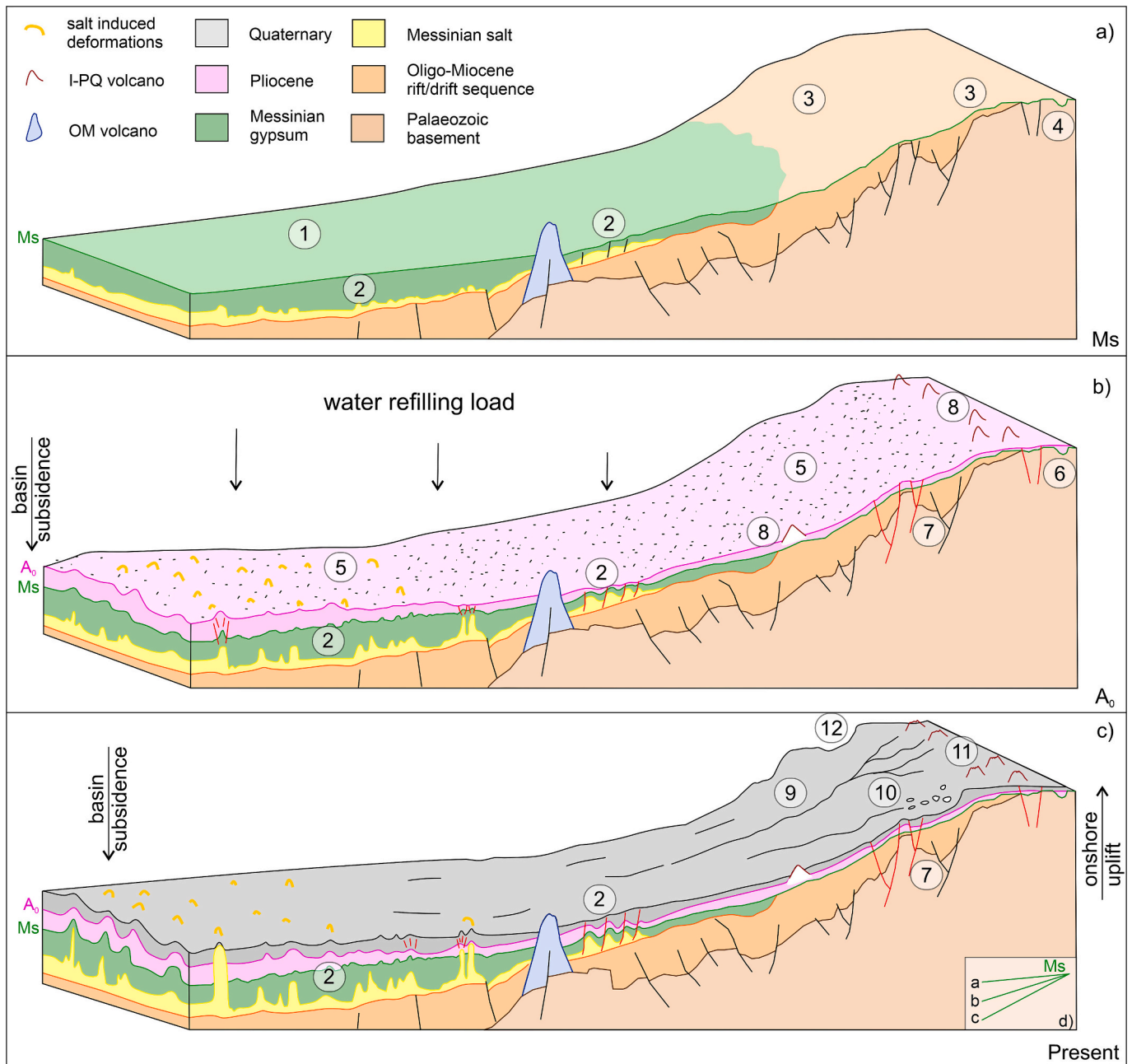
Fig. 14. Tectono-sedimentary evolution of the West Sardinian margin, a) at the end of the Messinian, b) at the end of the Pliocene, c) at the present-day. 1 = Messinian deposits in the lower slope and basin, 2 = Halokinetic processes in lower slope and deep basin, 3 = Messinian erosion in the shelf and upper slope, 4 = Messinian canyon, 5 = Pliocene deposition, 6 = Messinian canyon filled, 7 = Fault activity, 8 = Volcanoes developing on shelf and slope, 9 = Canyon activity, 10 = Pockmarks, 11 = Erosion of volcanoes peaks, 12 = Clinoforms. In panel d) a qualitative sketch of the Ms dip variation at the three timeframes due to basin subsidence and onshore uplift during the PQ.

following the opening of the Western Mediterranean and the post-Messinian water reload. The maximum salt tectonic activity occurred during the Pliocene, when subsidence and water loading effects were at their peak. However, salt-driven tectonics continued throughout the Quaternary (Figs. 2, 3, 4 and 14; Table 2e, f), as testified by the deformation of the Quaternary unit (Figs. 2, 6b and 8a2; Table 2e). Evidence of seafloor deformation and of diapirs outcropping at the seafloor (Fig. 1) near the Gulf of Lion further supports ongoing halokinetic activity during this period.

Fluid migration is another factor affecting the dynamics of the region. Recent normal faults and microfractures associated with pre-Pliocene sequences act as conduits for gas upwelling, as evidenced by seismic signal blanking and the formation of pockmarks on the seafloor

and in the PQ sequence (Løseth et al., 2003). These fluid escape structures appear closely linked to canyon pathways in the southern tilted outer shelf (Fig. 10, 14c, S4a). Several pockmarks emerging on the seafloor appear to have locally contributed to canyon paths, as highlighted in Figs. 10, 14c and S4a for the OCS and as already described by Cabrera et al. (2024) for the Blanes Canyon in the Catalan margin.

5.5. Plio-Quaternary sediment dynamics

Sedimentation patterns on the West Sardinian continental margin have been influenced by the interplay between tectonic and magmatic activity, sea-level changes and sediment sources during the PQ. The Pliocene depocenter is concentrated near the Gulf of Oristano (Fig. 6c),

fed by the Tirso River, which is the primary sediment source in the region (Fadda and Pala, 1992; Barrocu et al., 2004). In contrast, Pliocene sediments are thin or absent north of the Gulf, where no major rivers contribute with sediments to marine deposition. Here, the steepness of the foresets may have contributed to mass-wasting processes, as indicated by chaotic units at the foot of clinoforms (Fig. 12a) (Mulder, 2011; Felix and McCaffrey, 2005). The Pliocene oblique reflections on the outer continental shelf and upper slope (Fig. 12b, c), indicate higher sediment supply (Pirmez et al., 1998), likely driven by the growing tilting of the margin. During the Quaternary, the main depocenter is represented by the filling of the OCS-b and c branches (Fig. 11d) on the continental shelf. The regressive clinoform system (Fig. 2a, 12), exhibiting a sigmoidal geometry, probably formed during the late Pleistocene in response to the seaward migration of the coastline during the high-amplitude glacio-eustatic sea-level falls that characterized the period (Aiello, 2022). The observed variability in the distance between the shelf break and the offlap break seems to be conditioned by an uneven coastal erosion and related sediment supply. It is more prominent north of the Gulf of Oristano (Fig. 12a), due to the onshore uplift (Cocco et al., 2013, 2019), which favored high sediment flux resulting in higher clinoforms (Carvajal et al., 2009). Conversely, in front of the Gulf of Oristano, the clinoforms are thinner and shorter (Fig. 12b, c), likely because sediment was diverted by the OCS, which prevented accumulation at the foresets and limited clinoform growth (Patruno and Helland-Hansen, 2018). Furthermore, the widespread truncation of volcanic peaks observed in the shelf (Fig. S3) points to a dominance of seafloor erosion, probably during those sea level falls and lowstand stages, and likely sediment-starved environment. Canyon systems, a key feature in shaping the margin, developed during the Quaternary (Figs. 10, 11). These canyons, classified as Type 2 (Harris and Whiteway, 2011), primarily incise the Quaternary sequence but locally reach the Messinian unit where PQ deposits are thinner. While Harris and Whiteway (2011) and Migeon et al. (2012) suggested that canyon pathways in the western Mediterranean are controlled by Messinian pre-existing topography, this is not the case for the West Sardinian margin. Here, the canyons seem to develop more recently, given that they generally only erode the Quaternary sediments (Fig. 11). In some cases, the truncation of PQ reflections is observed, along with filling facies within the canyons, likely corresponding to Quaternary deposits (Table 2b). This suggests that, while the majority of canyon only erode the Quaternary deposits, locally a few reach the Ms horizon in recent times (Table 2b). We hypothesize that the ongoing tilting of the margin and the high amplitude frequency of the Quaternary glacio-eustatic sea level falls (Chiocci et al., 1997; Ercilla et al., 2021) likely favored the occurrence of sediment gravity instability processes along those canyons (Lo Iacono et al., 2014). This is because the rate of sediment supply increases, favored by the sea level falls and the erosion of the onshore uplifted areas (Miller, 2009; Piper and Normark, 2009), and deposition occurs on a quasi-continuous over steepening of the entire margin, reducing the stability of the canyon near-surface sediments. These processes likely accelerated canyon formation, with sediment erosion and deposition shaping the modern landscape.

6. Conclusions

The evolution of the West Sardinian continental margin and adjacent basin during the PQ is characterized by the interplay of tectonic, sedimentary, magmatic, and fluid dynamic processes. Our investigation, based on the analysis of both old and recent seismic profiles, provides new insights into the tectono-sedimentary processes that have shaped these regions. We refine the Plio-Quaternary stratigraphy with the identification of the A_0 reflector, interpreted as the base of the Quaternary (ca. 2.6 Ma), that allows us to subdivide the Pliocene and Quaternary units based on distinct seismic facies, which mirrors pattern observed in other Mediterranean basins.

Several significant geological structures and features affecting the

geometry, lateral continuity and distribution of Pliocene and Quaternary deposits have been identified. They include: a) salt tectonic structures in the lower continental slope and deep basin, b) normal faulting in the continental shelf and slope, c) volcanoes on the continental shelf and slope, and at the slope and deep basin boundary, d) pockmarks in the shelf and upper slope, e) canyon systems and canyon fill deposits in the slope, with many canyon heads indenting the shelf, and f) a regressive clinoform system on the shelf.

The aforementioned structures have been correlated to several processes shaping the margin. Vertical movements, related to the Oligo-Miocene opening of the Sardo-Provençal basin, the loading/unloading effects of the MSC and the Pleistocene onshore uplift, have influenced the margin's tilting. These also affected the tectonic setting of the margin through Oligo-Miocene fault reactivations during the Plio-Quaternary. Faults frequently acted as pathways for both magmatic and fluid upwelling, leading to the formation of volcanic edifices and pockmarks. Magmatic activity was particularly active during the Pliocene, with volcanic structures distributed along the shelf and slope. Magmatic edifices, along with halokinetic processes driven by salt tectonics, have significantly influenced sediment deposition and deformation. While halokinetic activity was most pronounced during the Pliocene, evidence of ongoing deformation at the seafloor, particularly towards the Gulf of Lion, suggests that these processes are still active today. The tilting of the margin, combined with sediment supply from onshore sources, drove the formation of clinoforms and the development of canyons that shaped the margin's current morphology. The evidence suggests that margin tilting, in combination with high-frequency sea-level falls during the Quaternary, led to gravity-driven sediment instability, accelerating canyon formation and contributing to the sedimentary architecture of the region. Studying the tectono-sedimentary processes affecting the two units of the PQ sequence provides a solid basis for future comparison with other Mediterranean margins, contributing to a more comprehensive understanding of their regional geological evolution.

Supplementary data to this article can be found online at https://doi.org/10.1016/j.margeo.2024.107450.

CRediT authorship contribution statement

Veronica Frisicchio: Writing – original draft, Visualization, Methodology, Formal analysis, Data curation, Conceptualization, Writing – review & editing. **Anna Del Ben:** Writing – review & editing, Visualization, Supervision, Methodology, Conceptualization. **Riccardo Geletti:** Writing – review & editing, Resources, Data curation. **Maria Cristina Caradonna:** Visualization. **Michele Rebesco:** Writing – review & editing. **Massimo Bellucci:** Writing – review & editing, Resources.

Declaration of competing interest

The authors declare that they have no known competing financial interests or personal relationships that could have appeared to influence the work reported in this paper.

Data availability

The seismic data are available at the Seismic data Network Access Point (SNAP). URL: https://snap.ogs.trieste.it/

framework of the European Marine Observation and Data Network (EMODnet) Geology Project for the profitable discussions.

We would like to sincerely thank the editor Gemma Ercilla, the reviewer Jesus Galindo-Zaldivar and an anonymous reviewer for the constructive suggestions that greatly improved the quality of our manuscript.

References

Aiello, G., 2022. Quaternary Lowstand Prograding Wedges of the Salento Continental Shelf (Southern Adriatic Sea, Italy): architectural Stacking patterns and the control of Glacio-Eustatic Sea Level Fluctuations and Foreland Tectonic Uplift. Geosciences 13 (1), 4. https://doi.org/10.3390/geosciences13010004.

Barca, S., Patta, E.D., Murtas, M., Pisanu, G., Serra, M., Lecca, L., De Muro, S., Pascucci, V., Carboni, S., Tilocca, G., Andreucci, S., Pusceddu, N., 2016. Note Illustrative della Carta geologica d'Italia alla scala 1:50.000, F. 528 Oristano, Servizio Geologico d'Italia - ISPRA. https://doi.org/10.15161/oar.it/143411.

Barrocu, G., Vernier, A., Ardau, F., Salis, N., Sanna, F., Sciabica, M.G., Soddu, S., 2004. Hydrogeology of the Island of Sardinia - Volume 5 from P37 to P54. In: Presented at the 32nd International Geological Congress.

Bellucci, M., Aslanian, D., Moulin, M., Rabineau, M., Leroux, E., Pellen, R., Poort, J., Del Ben, A., Gorini, C., Camerlenghi, A., 2021a. Salt morphologies and crustal segmentation relationship: new insights from the Western Mediterranean Sea. Earth Sci. Rev. 222, 103818. https://doi.org/10.1016/j.earscirev.2021.103818.

Bellucci, M., Pellen, R., Leroux, E., Bache, F., Garcia, M., Do Couto, D., Raad, F., Blondel, S., Rabineau, M., Gorini, C., Moulin, M., Maillard, A., Lofi, J., Del Ben, A., Camerlenghi, A., Poort, J., Aslanian, D., 2021b. A Comprehensive and Updated Compilation of the Seismic Stratigraphy Markers in the Western Mediterranean Sea. https://doi.org/10.17882/80128.

Bellucci, M., Leroux, E., Aslanian, D., Moulin, M., Pellen, R., Rabineau, M., 2024. Salt tectonics evolution in the Provençal Basin, Western Mediterranean Sea. BSGF-Earth Sci. Bull. 195, 16.

Bigi, G., Coli, M., Cosentino, D., Dal Piaz, G.V., Parotto, M., Sartori, R., Scandone, P., 1992a. Structural Model of Italy scale 1:500.000, sheet 3. In: C.N.R. Progetto Finalizzato Geodinamica, SELCA Firenze.

Bigi, G., Cosentino, D., Parotto, M., Sartori, R., Scandone, P., 1992b. Structural Model of Italy scale 1:500.000, sheet 5. In: C.N.R. Progetto Finalizzato Geodinamica, SELCA Firenze.

Brun, J.-P., Fort, X., 2011. Salt tectonics at passive margins: geology versus models. Mar. Pet. Geol. 28, 1123–1145. https://doi.org/10.1016/j.marpetgeo.2011.03.004.

Brun, J.-P., Mauduit, T.P.-O., 2008. Rollovers in salt tectonics: the inadequacy of the listric fault model. Tectonophysics 457, 1–11. https://doi.org/10.1016/j.tecto.2007.11.038.

Cabrera, A., Puig, P., Durán, R., Fabri, M.-C., Guerin, C., Lo Iacono, C., Huvenne, V.A.I., 2024. Geomorphology and evolution of the Blanes Canyon (NW Mediterranean). new insights from high resolution mapping of vertical cliffs. Geomorphology 461, 109290. https://doi.org/10.1016/j.geomorph.2024.109290.

Carmignani, L., Oggiano, G., Funedda, A., Conti, P., Pasci, S., 2016. The geological map of Sardinia (Italy) at 1:250,000 scale. J. Maps 12, 826–835. https://doi.org/10.1080/17445647.2015.1084544.

Carminati, E., Lustrino, M., Doglioni, C., 2012. Geodynamic evolution of the central and western Mediterranean: Tectonics vs. igneous petrology constraints. Tectonophysics 579, 173–192. https://doi.org/10.1016/j.tecto.2012.01.026.

Carvajal, C., Steel, R., Petter, A., 2009. Sediment supply: the main driver of shelf-margin growth. Earth Sci. Rev. 96 (4), 221–248. https://doi.org/10.1016/j.earscirev.2009.06.008.

Casula, G., Cherchi, A., Montadert, L., Murru, M., Sarria, E., 2001. The Cenozoic graben system of Sardinia (Italy): geodynamic evolution from new seismic and ®eld data. Mar. Pet. Geol. 32. https://doi.org/10.1016/S0264-8172(01)00023-X.

Cherchi, A., Montadert, L., 1982. Oligo-Miocene rift of Sardinia and the early history of the Western Mediterranean Basin. Nature 298, 736–739. https://doi.org/10.1038/298736a0.

Cherchi, A., Marcello, A., Marini, A., Murru, M., Pretti, S., Salvadori, I., 1982. Carta Geologica della Sardegna (1:250.000) London: Ente Minerario Sardo. Istituto di Geologia, Università di Cagliari.

Cherchi, A., Mancin, N., Montadert, L., Murru, M., Putzu, M.T., Schiavinotto, F., Verrubbi, V., 2008. The stratigraphic response to the Oligo-Miocene extension in the western Mediterranean from observations on the Sardinia graben system (Italy). Bull. Soc. Géol. Fr. 179, 267–287. https://doi.org/10.2113/gssgfbull.179.3.267.

Chiocci, F.L., Ercilla, G., Torre, J., 1997. Stratal architecture of Western Mediterranean Margins as the result of the stacking of Quaternary lowstand deposits below 'glacio-eustatic fluctuation base-level. Sediment. Geol. 112, 195–217. https://doi.org/10.1016/S0037-0738(97)00035-3.

CIESM, 2008. The Messinian Salinity Crisis from mega-deposits to microbiology — a consensus report. In: Briand, F. (Ed.), Workshop Monographs, Vol. 33 (168 pp.).

Civile, D., Lodolo, E., Alp, H., Ben-Avraham, Z., Cova, A., Baradello, L., Accettella, D., Burca, M., Centonze, J., 2014. Seismic stratigraphy and structural setting of the Adventure Plateau (Sicily Channel). Mar. Geophys. Res. 35, 37–53. https://doi.org/10.1007/s11001-013-9205-5.

Clauzon, G., Suc, J.-P., Gautier, F., Berger, A., Loutre, M.-F., 1996. Alternate interpretation of the Messinian salinity crisis: controversy resolved? Geol 24, 363. https://doi.org/10.1130/0091-7613(1996)024<0363:AIOTMS>2.3.CO;2.

Cocco, F., 2013. Plio-Pleistocene Tectonic Evolution of Southern Sardinia (Doctoral dissertation).. Università degli Studi di Cagliari.

Cocco, F., Funedda, A., Patacca, E., Scandone, P., 2013. Plio-Pleistocene extensional tectonics in the Campidano graben (SW Sardinia, Italy): preliminary note. Rend. Online Soc. Geol. It. 29, 31–34.

Cocco, F., Andreucci, S., Sechi, D., Cossu, G., Funedda, A., 2019. Upper Pleistocene tectonics in western Sardinia (Italy): Insights from the Sinis peninsula structural high. Terra Nova 31, 485–493. https://doi.org/10.1111/ter.12418.

Coltorti, M., Pieruccini, P., Montagna, P., Zorzi, F., 2015. Stratigraphy, facies analysis and chronology of Quaternary deposits at Capo S. Marco (Sinis Peninsula, West Sardinia, Italy). In: Quaternary International, Correlations of Quaternary Fluvial, Eolian, Deltaic and Marine Sequences 2013, Vol. 357, pp. 158–175. https://doi.org/10.1016/j.quaint.2014.03.033.

Conforti, A., Budillon, F., Tonielli, R., Falco, G.D., 2016. A newly discovered Pliocene volcanic field on the western Sardinia continental margin (western Mediterranean). Geo-Mar. Lett. 36, 1–14. https://doi.org/10.1007/s00367-015-0428-0.

Dal Cin, M., Del Ben, A., Mocnik, A., Accaino, F., Geletti, R., Wardell, N., Zgur, F., Camerlenghi, A., 2015. Seismic imaging of late Miocene (Messinian) evaporites from Western Mediterranean back-arc basins. Pet. Geosci. 22, 297–308. https://doi.org/10.1144/petgeo2015-096.

De Falco, G., Carannante, A., Del Vais, C., Gasperini, L., Pascucci, V., Sanna, I., Simeone, S., Conforti, A., 2022. Evolution of a single incised valley related to inherited geology, sea level rise and climate changes during the Holocene (Tirso river, Sardinia, western Mediterranean Sea). Mar. Geol. 451, 106885. https://doi.org/10.1016/j.margeo.2022.106885.

Deiana, G., Lecca, L., Melis, R., Soldati, M., Demurtas, V., Orrù, P., 2021. Submarine Geomorphology of the Southwestern Sardinian Continental Shelf (Mediterranean Sea): Insights into the last Glacial Maximum Sea-Level changes and Related Environments. Water 13, 155. https://doi.org/10.3390/w13020155.

Del Ben, A., Mocnik, A., Camerlenghi, A., Geletti, R., Zgur, F., 2018. 9. A, B, D, D - Eastern Sardo-Provençal Basin. In: Lofi, J. (Ed.), Seismic Atlas of the Messinian salinity crisis markers in the Mediterranean sea. Volume 2, Mem. Soc. géol. fr., n.s, 2018, t 181, and Commission for the Geological Map of the World, pp. 33–37. https://doi.org/10.10682/2018MESSINV2.

Dewey, J.F., Helman, M.L., Turco, E., Hutton, D.H.W., Knott, S.D., 1989. Kinematics of the western Mediterranean. Geol. Soc. Lond. Spec. Publ. 45, 265–283. https://doi.org/10.1144/GSL.SP.1989.045.01.15.

Dos Reis, A.T., Gorini, C., Mauffret, A., 2005. Implications of salt–sediment interactions on the architecture of the Gulf of Lions deep-water sedimentary systems—western Mediterranean Sea. In: Marine and Petroleum Geology, The Gulf of Lions: An Overview of Recent Studies within the French "Margins" Programme, 22, pp. 713–746. https://doi.org/10.1016/j.marpetgeo.2005.03.006.

EMODnet, 2016. EMODNET Bathymetry Consortium, 2016. EMODNET Digital Bathymetry. European Marine Observation and Data Network (EMODnet). URL. https://emodnet.ec.europa.eu/en/bathymetry (accessed 7.26.23).

Ercilla, G., Vázquez, J.T., Alonso, B., et al., 2021. Chapter 6: Seafloor morphology and processes in the Alboran Sea. In: Báez, J.C., Vázquez, J.T., et al. (Eds.), Alboran Sea - Ecosystems and Marine Resources. Springer Nature Switzerland AG, pp. 157–205. https://doi.org/10.1007/978-3-030-65516-7_6.

Ercilla, G., Galindo-Zaldívar, J., Estrada, F., Valencia, J., Juan, C., Casas, D., Alonso, B., Comas, M.C., Tendero-Salmerón, V., Casalbore, D., Azpiroz-Zabala, M., Bárcenas, P., Ceramicola, S., Chiocci, F.L., Idárraga-García, J., López-González, N., Mata, P., Palomino, D., Rodríguez-García, J.A., Teixeira, M., Nespereira, J., Vázquez, J.T., Yenes, M., 2022. Understanding the complex geomorphology of a deep sea area affected by continental tectonic indentation: the case of the Gulf of Vera (Western Mediterranean). Geomorphology 402, 108126. https://doi.org/10.1016/j.geomorph.2022.108126.

Estrada, F., Ercilla, G., Gorini, C., Alonso, B., Vázquez, J.T., García-Castellanos, D., Juan, C., Maldonado, A., Ammar, A., Elabbassi, M., 2011. Impact of pulsed Atlantic water inflow into the Alboran Basin at the time of the Zanclean flooding. Geo-Mar. Lett. 31, 361–376. https://doi.org/10.1007/s00367-011-0249-8.

Fabbri, A., Nanni, T., 1980. Seismic Reflexion Study of the Sardinia Basin (Tyrrhenian Sea). https://doi.org/10.3406/geolm.1980.1137.

Faccenna, C., Speranza, F., Caracciolo, F.D., Mattei, M., Oggiano, G., 2002. Extensional tectonics on Sardinia (Italy): insights into the arc–back-arc transitional regime. Tectonophysics 356, 213–232. https://doi.org/10.1016/S0040-1951(02)00287-1.

Fadda, A.F., Pala, A., 1992. Le acque della Sardegna. Co Edi Sar - Cagliari.

Fais, S., Klingele, E.E., Lecca, L., 1996. Oligo-Miocene half graben structure in Western Sardinian Shelf (western Mediterranean): reflection seismic and aeromagnetic data comparison. Mar. Geol. 133, 203–222. https://doi.org/10.1016/0025-3227(96)00030-8.

Felix, M., McCaffrey, W., 2005. SEDIMENTARY PROCESSES | particle-driven subaqueous gravity processes. In: Encyclopedia of Geology. Elsevier, pp. 1–7. https://doi.org/10.1016/B0-12-369396-9/00484–6.

Ferrandini, J., Gattacceca, J., Ferrandini, M., Deino, A., Janin, M.C., 2003. Chronostratigraphie et paléomagnétisme des dépôts oligo-miocènes de Corse: implications géodynamiques pour l'ouverture du bassin liguro-provençal. Bull. Soc. Geol. Fr. 174, 357–371.

Finetti, I., Morelli, C., 1974. Esplorazione geofisica dell'area mediterranean circostante il blocco Sardo-Corso. In: In "Paleogeografia del Terziario sardo nell'ambito del Mediterraneo occidentale" suppl. ai "Rendiconti del Seminario della Facoltà di Scienze dell'Università di Cagliari". Graficoop -Soc. Tipografica Editoriale, Bologna.

Finetti, I., Del Ben, A., Fais, S., Forlin, E., Klingele, E.E., Lecca, L., Pipan, M., Prizzon, A., 2005. Crustal tectono-stratigraphic setting and geodynamics of the corso-sardinian block from new CROP seismic data. In: Finetti, I. (Ed.), CROP PROJECT: Deep

Seismic Exploration of the Central Mediterranean and Italy. Atlases in Geoscience, 1. Elsevier B.V., pp. 430–446

Franciosi, L., Lustrino, M., Melluso, L., Morra, V., D'Antonio, M., 2003. Geochemical characteristics and mantle sources of the Oligo-Miocene primitive basalts from Sardinia: the role of subduction components. Ofioliti 28, 105–114. https://doi.org/10.4454/ofioliti.v28i2.198.

Frisicchio, V., Del Ben, A., Bellucci, M., Blondel, S., Camerlenghi, A., Geletti, R., 2023. Non-Real but Realistic Distribution of Small High-Frequency Structures in 2D Seismic Data. Presented at the GNGTS. https://doi.org/10.13120/2tf2-1j75.

Funedda, A., Pertusati, P.C., Carmignani, L., Uras, V., Pisanu, G., Murtas, M., 2012. Note illustrative della Carta Geologica d'Italia 1:50.000 "Foglio 540 - Mandas".

Garcia-Castellanos, D., Villaseñor, A., 2011. Messinian salinity crisis regulated by competing tectonics and erosion at the Gibraltar arc. Nature 480, 359–363. https://doi.org/10.1038/nature10651.

Gargani, J., 2004. Modelling of the erosion in the Rhone valley during the Messinian crisis (France). Q. Int. Adv. Quat. Stud. 121, 13–22. https://doi.org/10.1016/j.quaint.2004.01.020.

Gargani, J., Rigollet, C., Scarselli, S., 2010. Isostatic response and geomorphological evolution of the Nile valley during the Messinian salinity crisis. Bull. Soc. Géol. Fr. 181, 19–26. https://doi.org/10.2113/gssgfbull.181.1.19.

Gattacceca, J., Deino, A., Rizzo, R., Jones, D.S., Henry, B., Beaudoin, B., Vadeboin, F., 2007. Miocene rotation of Sardinia: New paleomagnetic and geochronological constraints and geodynamic implications. Earth Planet. Sci. Lett. 19. https://doi.org/10.1016/j.epsl.2007.02.003.

Gaullier, V., Loncke, L., Vendeville, B., Déverchère, J., Droz, L., 2007. Salt Tectonics in the Deep Mediterranean: Indirect Clues for Understanding the Messinian Salinity Crisis.

Geletti, R., Zgur, F., Del Ben, A., Buriola, F., Fais, S., Fedi, M., Forte, E., Mocnik, A., Paoletti, V., Pipan, M., Ramella, R., Romeo, R., Romi, A., 2014. The Messinian Salinity Crisis: new seismic evidence in the West-Sardinian margin and Eastern Sardo-Provençal basin (West Mediterranean Sea). Mar. Geol. 351, 76–90. https://doi.org/10.1016/j.margeo.2014.03.019.

Govers, R., Meijer, P., Krijgsman, W., 2009. Regional isostatic response to Messinian Salinity Crisis events. Tectonophysics 463, 109–129. https://doi.org/10.1016/j.tecto.2008.09.026.

Guennoc, P., Gorini, C., Mauffret, A., 2000. Histoire géologique du Golfe du Lion et Cartographie du Rift Oligo-Aquitanien et de la Surface Messinienne* Geological History of the Gulf of Lions: Mapping the Oligocene-Aquitanian Rift and Messinian Surface.

Haq, B.U., Hardenbol, J., Vail, P.R., 1987. Chronology of Fluctuating Sea Levels since the Triassic. Science 235, 1156–1167. https://doi.org/10.1126/science.235.4793.1156.

Harris, P.T., Whiteway, T., 2011. Global distribution of large submarine canyons: Geomorphic differences between active and passive continental margins. Mar. Geol. 285, 69–86.

Heida, H., Raad, F., Garcia-Castellanos, D., Jiménez- Munt, I., Maillard, A., Lofi, J., 2022. Flexural-isostatic reconstruction of the Western Mediterranean during the Messinian Salinity Crisis: Implications for water level and basin connectivity. Basin Res. 34, 50–80. https://doi.org/10.1111/bre.12610.

Horni, J., Geissler, W.H., Doornenbal, H., Gaina, C., 2014. Offshore volcanic facies. In: Hopper, J.R., Funck, T., Stoker, M.S., Árting, U., Peron-Pinvidic, G. (Eds.), Tectonostratigraphic Atlas of the North-East Atlantic Region. Geological Survey of Denmark and Greenland (GEUS), Copenhagen, Denmark, pp. 235–253.

Horni, J., Hopper, J., Blischke, A., Geisler, W., Stewart, M., McDermott, K., Judge, M.T., Erlendsson, Ö., Árting, U., 2017. Regional distribution of volcanism within the North Atlantic Igneous Province. Geol. Soc. Lond. Spec. Publ. 447 (SP447), 18. https://doi.org/10.1144/SP447.18.

Hsü, K.J., Cita, M.B., Ryan, W.B.F., 1973. The Origin of the Mediterranean Evaporites. DSDP Initial Reports XIII.

Juan, C., Ercilla, G., Javier Hernández-Molina, F., Estrada, F., Alonso, B., Casas, D., García, M., Farran, M., Llave, E., Palomino, D., Vázquez, J.-T., Medialdea, T., Gorini, C., D'Acremont, E., El Moumni, B., Ammar, A., 2016. Seismic evidence of current-controlled sedimentation in the Alboran Sea during the Pliocene and Quaternary: Palaeoceanographic implications. Mar. Geol. 378, 292–311. https://doi.org/10.1016/j.margeo.2016.01.006. The contourite log-book: significance for palaeoceanography, ecosystems and slope instability.

Kallweit, R.S., Wood, L.C., 1982. The limits of resolution of zero-phase wavelets. GEOPHYSICS 47, 1035–1046. https://doi.org/10.1190/1.1441367.

Krijgsman, W., Hilgen, F.J., Raffi, I., Sierro, F.J., Wilson, D.S., 1999. Chronology, causes and progression of the Messinian Salinity Crisis. Nature 400, 652–655. https://doi.org/10.1038/23231.

Lecca, L., 2000. La piattaforma continentale miocenico-quaternaria del margine occidentale sardo: blocco diagramma sezionato. Rend. Semin. Fac. Sci. Univ. Cagliari 1, 49–70.

Leroux, E., Rabineau, M., Aslanian, D., Gorini, C., Molliex, S., Bache, F., Robin, C., Droz, L., Moulin, M., Poort, J., Rubino, J.-L., Suc, J.-P., 2017. High-resolution evolution of terrigenous sediment yields in the Provence Basin during the last 6 Ma: relation with climate and tectonics. Basin Res. 29, 305–339. https://doi.org/10.1111/bre.12178.

Lo Iacono, C., Sulli, A., Agate, M., 2014. Submarine canyons of North-Western Sicily (Southern Tyrrhenian Sea): variability in morphology, sedimentary processes and evolution on a tectonically active margin. Deep-Sea Res. II Top. Stud. Oceanogr. 104, 93–105. https://doi.org/10.1016/j.dsr2.2013.06.018.

Lofi, J., 2018. Seismic Atlas of the Messinian salinity crisis markers in the Mediterranean sea. In: Volume 2 - Mem. Soc. géol. fr., n.s., 2018, t. 181, and Commission for the Geological Map of the World, 72. https://doi.org/10.10682/2018MESSINV2.

Lofi, J., Gorini, C., Berné, S., Clauzon, G., Tadeu Dos Reis, A., Ryan, W.B.F., Steckler, M. S., 2005. Erosional processes and paleo-environmental changes in the Western Gulf of Lions (SW France) during the Messinian Salinity Crisis. Mar. Geol. 217, 1–30. https://doi.org/10.1016/j.margeo.2005.02.014.

Lofi, J., Déverchère, J., Gorini, C., Gaullier, V., Herve, G., Guennoc, P., Loncke, L., Maillard, A., Sage, F., Thinon, I., 2007. The Messinian Salinity Crisis in the offshore domain: an overview of our knowledge through seismic profile interpretation and multi-site approach. In: CIESM Workshop Monographs, Vol. 33.

Lofi, J., Deverchère, J., Gaullier, V., Gillet, H., Gorini, C., Guennoc, P., Loncke, L., Maillard, A., Sage, F., Thinon, I., Capron, A., Obone Zue Obame, E., 2008. The Messinian Salinity Crisis in the Offshore Domain: An Overview of Our Knowledge Through Seismic Profile Interpretation and Multi-Site Approach CIESM Workshop Monographs, pp. 83–90.

Lofi, J., Déverchère, J., Gillet, H., Gorini, C., Guennoc, P., Loncke, L., Maillard, A., Sage, F., Thinon, I., 2011. Seismic Atlas of the Messinian Salinity Crisis Markers in the Mediterranean and Black Seas, Vol. 1. Memoire de la Société Géologique de France.

Loget, N., Van Den Driessche, J., 2006. On the origin of the Strait of Gibraltar. In: Sedimentary Geology, The Messinian Salinity Crisis Revisited 188–189, pp. 341–356. https://doi.org/10.1016/j.sedgeo.2006.03.012.

Løseth, H., Wensaas, L., Arntsen, B., Hovland, M., 2003. Gas and fluid injection triggering shallow mud mobilization in the Hordaland Group, North Sea. SP 216, 139–157. https://doi.org/10.1144/GSL.SP.2003.216.01.10.

Lustrino, M., Melluso, L., Morra, V., 2007a. The geochemical peculiarity of "Plio-Quaternary" volcanic rocks of Sardinia in the circum-Mediterranean area. Spec. Pap. Geol. Soc. Am. 418, 277–301. https://doi.org/10.1130/2007.2418(14).

Lustrino, M., Morra, V., Fedele, L., Serracino, M., 2007b. The transition between 'orogenic' and 'anorogenic' magmatism in the western Mediterranean area: the Middle Miocene volcanic rocks of Isola del Toro (SW Sardinia, Italy). Terra Nova 19, 148–159. https://doi.org/10.1111/j.1365-3121.2007.00730.x.

Lustrino, M., Fedele, L., Melluso, L., Morra, V., Ronga, F., Geldmacher, J., Duggen, S., Agostini, S., Cucciniello, C., Franciosi, L., Meisel, T., 2013. Origin and evolution of Cenozoic magmatism of Sardinia (Italy). A combined isotopic (Sr–Nd–Pb–O–Hf–Os) and petrological view. Lithos 180–181, 138–158. https://doi.org/10.1016/j.lithos.2013.08.022.

Mascarelli, A.L., 2009. Quaternary geologists win timescale vote. Nature 459, 624. https://doi.org/10.1038/459624a.

Mauffret, A., Contrucci, I., Brunet, C., 1999. Structural evolution of the Northern Tyrrhenian Sea from new seismic data. Mar. Pet. Geol. 16, 381–407. https://doi.org/10.1016/S0264-8172(99)00004-5.

Migeon, S., Mascle, J., Coste, M., Rouillard, P., 2012. Mediterranean submarine canyons and channels: Morphological and geological backgrounds. In: Mediterranean Submarine Canyons: Ecology and Governance. IUCN, Gland, Switzerland and Málllaga, Spain.

Miller, K.G., 2009. Sea Level Change, last 250 Million Years. In: Gornitz, V. (Ed.), Encyclopedia of Paleoclimatology and Ancient Environments. Encyclopedia of Earth Sciences Series. Springer, Dordrecht. https://doi.org/10.1007/978-1-4020-4411-3_206.

Mulder, T., 2011. Chapter 2 - Gravity processes and deposits on continental slope, rise and Abyssal plains. In: HüNeke, H., Mulder, T. (Eds.), Developments in Sedimentology, Deep-Sea Sediments. Elsevier, pp. 25–148. https://doi.org/10.1016/B978-0-444-53000-4.00002-0.

Norman, S.E., Chase, C.G., 1986. Uplift of the shores of the western Mediterranean due to Messinian desiccation and flexural isostasy. Nature 322, 450–451. https://doi.org/10.1038/322450a0.

Oudet, J., Münch, Ph., Verati, C., Ferrandini, M., Melinte-Dobrinescu, M., Gattacceca, J., Cornée, J.-J., Oggiano, G., Quillévéré, F., Borgomano, J., Ferrandini, J., 2010. Integrated chronostratigraphy of an intra-arc basin: 40Ar/39Ar datings, micropalaeontology and magnetostratigraphy of the early Miocene Castelsardo basin (northern Sardinia, Italy). Palaeogeogr. Palaeoclimatol. Palaeoecol. 295, 293–306. https://doi.org/10.1016/j.palaeo.2010.06.007.

Patruno, S., Helland-Hansen, W., 2018. Clinoforms and clinoform systems: Review and dynamic classification scheme for shorelines, subaqueous deltas, shelf edges and continental margins. Earth Sci. Rev. 185, 202–233. https://doi.org/10.1016/j.earscirev.2018.05.016.

Pellen, R., Aslanian, D., Rabineau, M., Suc, J.P., Gorini, C., Leroux, E., Blanpied, C., Silenziario, C., Popescu, S.M., Rubino, J.L., 2019. The Messinian Ebro River incision. Glob. Planet. Chang. 181, 102988. https://doi.org/10.1016/j.gloplacha.2019.102988.

Peterson, D.E., Garibaldi, N., Keranen, K., Tikoff, B., Miller, C., Lara, L.E., Tassara, A., Thurber, C., Lanza, F., 2020. Active Normal faulting, diking, and doming above the rapidly inflating Laguna del Maule Volcanic Field, Chile, Imaged with CHIRP, magnetic, and focal mechanism data. J. Geophys. Res. Solid Earth 125 (8). https://doi.org/10.1029/2019JB019329 e2019JB019329.

Piper, D.J.W., Normark, W.R., 2009. Processes that Initiate turbidity currents and their influence on Turbidites: a marine geology perspective. J. Sediment. Res. 79, 347–362. https://doi.org/10.2110/jsr.2009.046.

Pirmez, C., Pratson, L.F., Steckler, M.S., 1998. Clinoform development by advection-diffusion of suspended sediment: modeling and comparison to natural systems. J. Geophys. Res. Solid Earth 103 (B10), 24141–24157. https://doi.org/10.1029/98JB01516.

Planke, S., Symonds, P., Alvestad, E., Skogseid, J., 2000. Seismic volcanostratigraphy of large-volume basaltic extrusive complexes on rifted margins. J. Geophys. Res. Solid Earth 105, 19335–19351.

Rehault, J.-P., Boillot, G., Mauffret, A., 1984. The Western Mediterranean Basin geological evolution. Mar. Geol. 55, 447–477. https://doi.org/10.1016/0025-3227(84)90081-1.

Rehaut, J.P., 1981. thesis. Univ. Paris VI.

Rosenbaum, G., Lister, G.S., Duboz, C., 2002. Reconstruction of the tectonic evolution of the western Mediterranean since the Oligocene. J.Virt.Ex 08, 107–130. https://doi.org/10.3809/jvirtex.2002.00053.

Roveri, M., Flecker, R., Krijgsman, W., Lofi, J., Lugli, S., Manzi, V., Sierro, F.J., Bertini, A., Camerlenghi, A., De Lange, G., Govers, R., Hilgen, F.J., Hübscher, C., Meijer, P.Th., Stoica, M., 2014. The Messinian Salinity Crisis: past and future of a great challenge for marine sciences. Mar. Geol. 352, 25–58. https://doi.org/10.1016/j.margeo.2014.02.002, 50th Anniversary Special Issue.

Sage, F., Gronefeld, G.V., Deverchere, J., Gaullier, V., Maillard, A., Gorini, C., 2005. Seismic evidence for Messinian detrital deposits at the western Sardinia margin, northwestern Mediterranean. Mar. Pet. Geol. 17.

Savoye, B., Piper, D.J.W., 1991. The Messinian event on the margin of the Mediterranean Sea in the Nice area, southern France. Marine Geology 97, 279–304. https://doi.org/10.1016/0025-3227(91)90121-J.

Selli, R., Fabbri, A., 1971. Tyrrhenian: a Pliocene deep sea. Atti della Accademia Nazionale dei Lincei. Classe di Scienze Fisiche, Matematiche e Naturali. Rendiconti 50, 580–592.

Špelić, M., Del Ben, A., Petrinjak, K., 2021. Structural setting and geodynamics of the Kvarner area (Northern Adriatic). Mar. Pet. Geol. 125, 104857. https://doi.org/10.1016/j.marpetgeo.2020.104857.

Stampfli, G., Höcker, C., 1989. Messinian palaeorelief from 3-D seismic survey in the Tarraco concession area (Spanish Mediterranean Sea). Geol. Mijnb. 68, 201–210.

Torelli, L., Cornini, S., Brancolini, G., Zitellini, N., 1990. The Sardinia Channel (Central Mediterranean): a structural analysis of a submarine orogenic chain. Stud. Geol. Camerti Vol. Spec. 35–36.

Ulzega, A., 1988. Carta Geomorfologica della Sardegna marina e continentale. In: Geomorphological map of marine and continental Sardinia. Scala 1:500.000. Ist. Geogr. De Agostini, Novara.

ViDEPI project, 2009. Visibility of Petroleum Exploration Data in Italy. https://www.videpi.com/videpi/videpi.asp (accessed 20.01.2022).

Volpi, V., Del Ben, A., Civile, D., Zgur, F., 2017. Neogene tectono-sedimentary interaction between the Calabrian Accretionary Wedge and the Apulian Foreland in the northern Ionian Sea. Mar. Pet. Geol. 83, 246–260. https://doi.org/10.1016/j.marpetgeo.2017.03.013.

Würtz, M., Rovere, M., 2015. Atlas of the Mediterranean Seamounts and Seamount-like Structures. IUCN, Gland, Switzerland and Málaga, Spain, 276 pages.

Yilmaz, Ö., 2001. 3. Velocity Analysis and Statics Corrections. In: Seismic Data Analysis, Investigations in Geophysics. Society of Exploration Geophysicists, pp. 271–462. https://doi.org/10.1190/1.9781560801580.ch3.

Zgur, F., Geletti, R., Codiglia, R., Romeo, R., Accettella, D., Visnovic, P., Cappelli, G., Pasciullo, V., 2010. Sardegna Occidentale - Rapporto di Campagna c/r OGS Explora, 14.09–04.10.2010.